Marine and Petroleum Geology 114 (2020) 104209

Contents lists available at ScienceDirect

Marine and Petroleum Geology

journal homepage: www.elsevier.com/locate/marpetgeo

Research paper

Was volcanic activity during the Ordovician-Silurian transition in South China part of a global phenomenon? Constraints from zircon U–Pb dating of volcanic ash beds in black shales

Xuebin Du[a,b,*], Yongchao Lu[b], Dan Duan[a,b], Zhanhong Liu[a,b], Ke Zhao[a,b], Jixin Jia[a,b], Hang Fu[a]

[a] College of Marine Science and Technology, China University of Geoscience, Wuhan, 430074, China
[b] Key Laboratory of Tectonics and Petroleum Resources, China University of Geosciences, Ministry of Education, Wuhan, 430074, China

ARTICLE INFO

Keywords:
Volcanic ash
Black shales
Zircon
Hirnantian
Global stratigraphic correlation

ABSTRACT

Whether volcanic activity during the Ordovician-Silurian transition (OST) in South China (SC) contributed to global volcanic activity has always been a controversial subject. Volcanic ash is the most direct evidence for volcanic activity and represents a good marker to compare SC with the global stratigraphic correlation. Here, we analyze the distribution of volcanic ash beds in three outcrops in SC and precisely determine the ages of volcanic ash zircons using the LA-ICP-MS and SHRIMPII methods.

A comparison of the volcanic ash beds in three different outcrops of SC during the OST; indicates that relatively large-scale volcanic activity occurred during this period. The newly obtained zircon U–Pb ages show that the starting time of the Ordovician Wufeng Fm. was approximately 449.2 Ma (or 449.3 Ma), the starting time of the Ordovician Guanyingqiao bed (the ending time of the Wufeng Fm.) was approximately 445.6 Ma, and the starting time of the Longmaxi Fm. was approximately 444.2 Ma. In addition, the durations of the Wufeng Fm. and Guanyingqiao bed were 3.6 Ma and 1.4 Ma, respectively, and the duration of the Hirnantian stage in SC was 1.4 Ma. Most of the ages obtained in this study were basically consistent with that of the International Commission on Stratigraphy (GST 2018). These results provide insights into the volcanic activity during the OST in SC as well as age data for a global stratigraphic framework.

1. Introduction

The Ordovician-Silurian transition (OST) is an important geological interval. During which, global plate tectonics, paleoenvironments, paleoclimate, paleoredox conditions, and biological systems all underwent great changes, which directly led to changes in the global ecosystem (Kump and Arthur, 1999; Brenchley et al., 2003; Chen et al., 2006; Fan et al., 2009; Hammarlund et al., 2012; Shen et al., 2019; Wang et al., 2019a,2019b). At the same time, a set of black shales was deposited in South China (SC), which is an important target for commercial shale gas exploitation in China at present (Upper Ordovician Wufeng Formation, Lower Silurian Longmaxi Formation) (Yan et al., 2015a,2015b; Chen et al., 2016). This set of black shales contains a large number of graptolites and has numerous volcanic ash beds that have been altered to K-bentonite (Su et al., 2003, 2009). These features are regarded as good records for studying the key geological events during the transition from the Ordovician to Silurian.

Volcanic ash is the most direct evidence of volcanic activity during the OST and represents a good marker to compare SC with global stratigraphic correlations, and fossil evidence (Thompson et al., 2012; Svensen et al., 2015; Wu et al., 2018). Early scholars identified volcanic ash beds in the Upper Ordovician Wufeng Fm. in SC (Fu et al., 1983; Wang et al., 1983; Ross and Naeser, 1984; Huff et al., 1995; Chen et al., 2000). However, it was not until the early 21st century that studies on the distribution of volcanic ash beds and comparisons were carried out (Su et al., 2002; Yang et al., 2019). In recent years, researchers have begun to discuss the role of volcanic activity in the formation and enrichment of shale gas and have preliminarily suggested that volcanic activity exerts control over shale gas accumulation in SC (Lu et al., 2017; Shu et al., 2017; Wu et al., 2018).

An of the most important characteristic of volcanic ash is that it can contain a large number of zircons. Therefore, the precise ages of zircons can be used to determine and compare stratigraphic boundaries and timing of deposition. To date, few studies have performed zircon U–Pb dating of black shales from the Upper Ordovician Wufeng Fm. and Lower Silurian Longmaxi Fm. in SC. Initially, the SHRIMPII technique

* Corresponding author. College of Marine Science and Technology, China University of Geosciences, Wuhan, 430074, China.
E-mail addresses: basindu@163.com, basindu@gmail.com (X. Du).

https://doi.org/10.1016/j.marpetgeo.2019.104209
Received 5 October 2019; Received in revised form 24 December 2019; Accepted 26 December 2019
Available online 27 December 2019
0264-8172/

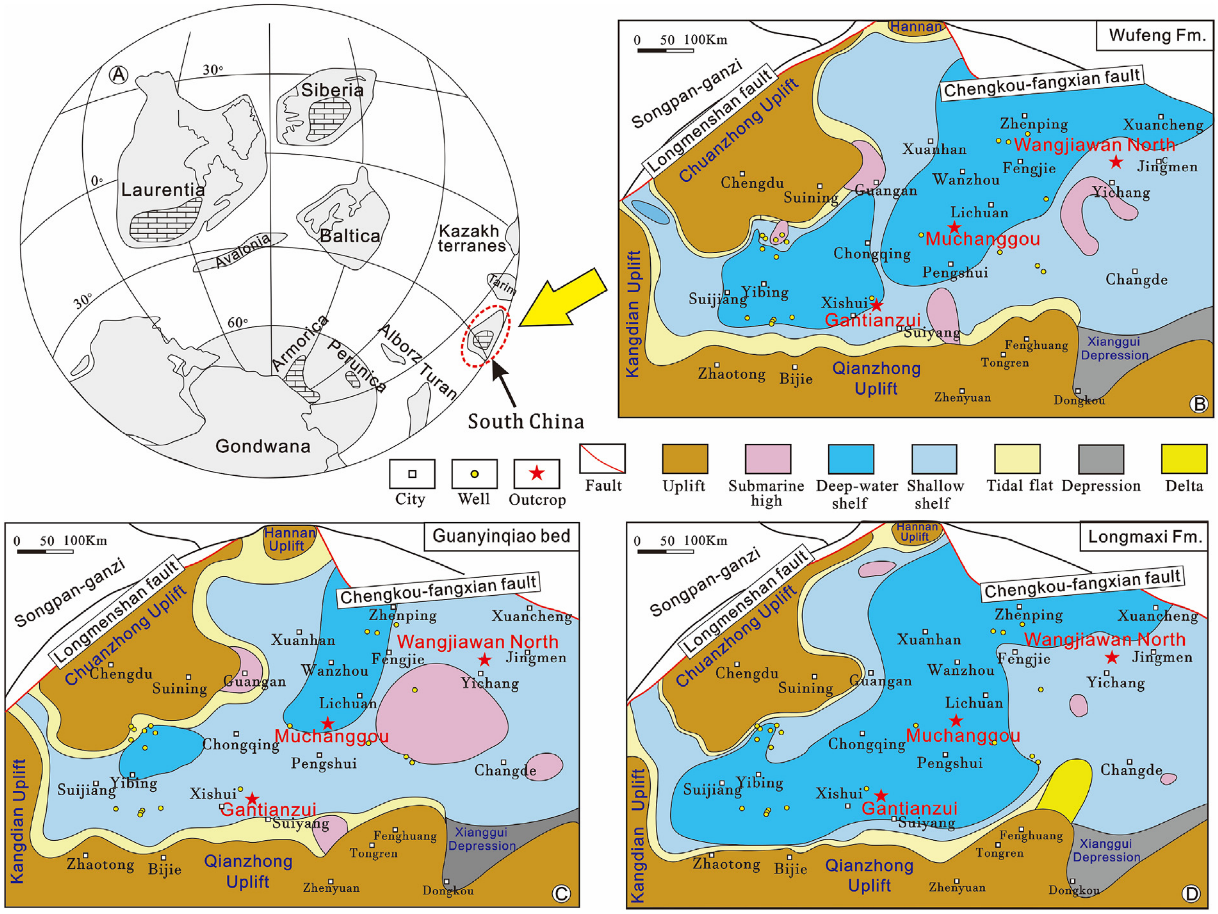

Fig. 1. (A) Paleogeographic reconstruction of the Late Ordovician (450 Ma) (modified from Huff et al., 2014). (B), (C), and (D) Maps displaying sedimentary lithofacies paleogeography of the Wufeng Fm. (448.3–445.2 Ma), Guanyingqiao bed (445.2–443.8 Ma), and the first member of the Longmaxi Fm. (443.8–438.5 Ma), respectively, in the Upper and Middle Yangtze regions, SC (lithofacies paleogeography is modified from Sun et al., 2018; Ages is referred by Lu et al., 2019).

was used to determine the age of volcanic ash zircons at the top of the Ordovician in the Wangjiawan outcrop, and it was dated to be approximately 443.2 ± 1.6 Ma (Hu et al., 2008). Subsequently, the age of volcanic ash zircons near the Ordovician-Silurian boundary in the Haoping outcrop in Hunan Province was obtained by the LA-ICP-MS method, and it was approximately 442.2 ± 8.1 Ma (Xie et al., 2012). The age of volcanic ash zircons in the early Silurian Longmaxi Fm. of the Mayangzhai outcrop is 450 ± 3.6 Ma (Luo et al., 2016). The age of the volcanic ash zircons in the middle and upper Shamao Fm. in the Qingyangba outcrop is 424.5 ± 6.4 Ma (Li et al., 2017). Obviously, these age data are different, which makes it difficult to establish an effective stratigraphic framework in SC and carry out regional and global stratigraphic correlations.

There are two possible reasons for the above different results. The first reason is limited by the amount of samples collected. Many samples of volcanic ash were collected in relatively small amounts (< 1 kg), resulting in an insufficient quantity of selected zircons and difficulty obtaining enough age data. The second reason is that different laboratories have different test methods and data processing procedures for zircon U–Pb dating, which leads to differences in the obtained age data. To address these problems, in this study, we collected large volcanic ash samples (each sample is greater than 3 kg) from three different outcrops in SC to ensure that enough zircons could be obtained. Second, to verify the reliability of the age data, in terms of testing methods, we used the LA-ICP-MS method and the SHRIMPII method separately to test the same sample, and compared the two age results. If the two ages are basically the same, the test method we adopted and the test results are reliable.

This study aims to achieve the following objectives: to obtain the precise age of zircons for the key interface of the OST in SC and provide insights into the stratigraphic correlation of the OST between the SC and GST 2018.

2. Geological setting

The Central and Upper Yangtze regions of SC are dominated by the Sichuan basin, including parts of Yunnan, Guizhou, Chongqing, Hubei and Hunan provinces, covering an area of approximately 35×10^4 km^2(Yan et al., 2015a,2015b; Chen et al., 2016). During the Late Ordovician-early Silurian period, SC was located near the paleoequator and belonged to the tropical and subtropical zone on the western margin of Gondwana (Fig. 1A) (Cocks, 2001; Huff et al., 2014). Due to the continuous expansion of the Qianzhong uplift, Kangdian uplift, Chuanzhong uplift, and Hannan uplift after the Middle Ordovician, the Yangtze platform gradually became a semiconfined shallow sea basin (Sun et al., 2018). At the same sedimentary time, the sedimentary backgrounds and lithological assemblages of the Middle and Upper Yangtze areas were basically the same, and no great change was observed (Fig. 1).

The OST period covers the Late Ordovician Katian and Hirnantian stages to the early Silurian Rhuddanian stage, and it includes the Upper Ordovician Wufeng Fm., Guanyinqiao bed and the Silurian Longmaxi Formation. In the Wufeng Fm., the sedimentary environment changed from a gentle carbonate slope to a fine-grained shale sedimentary system, which was located in a relatively deep-water area of a shallow epicontinental sea, and successively developed paleo-uplift, tidal flat

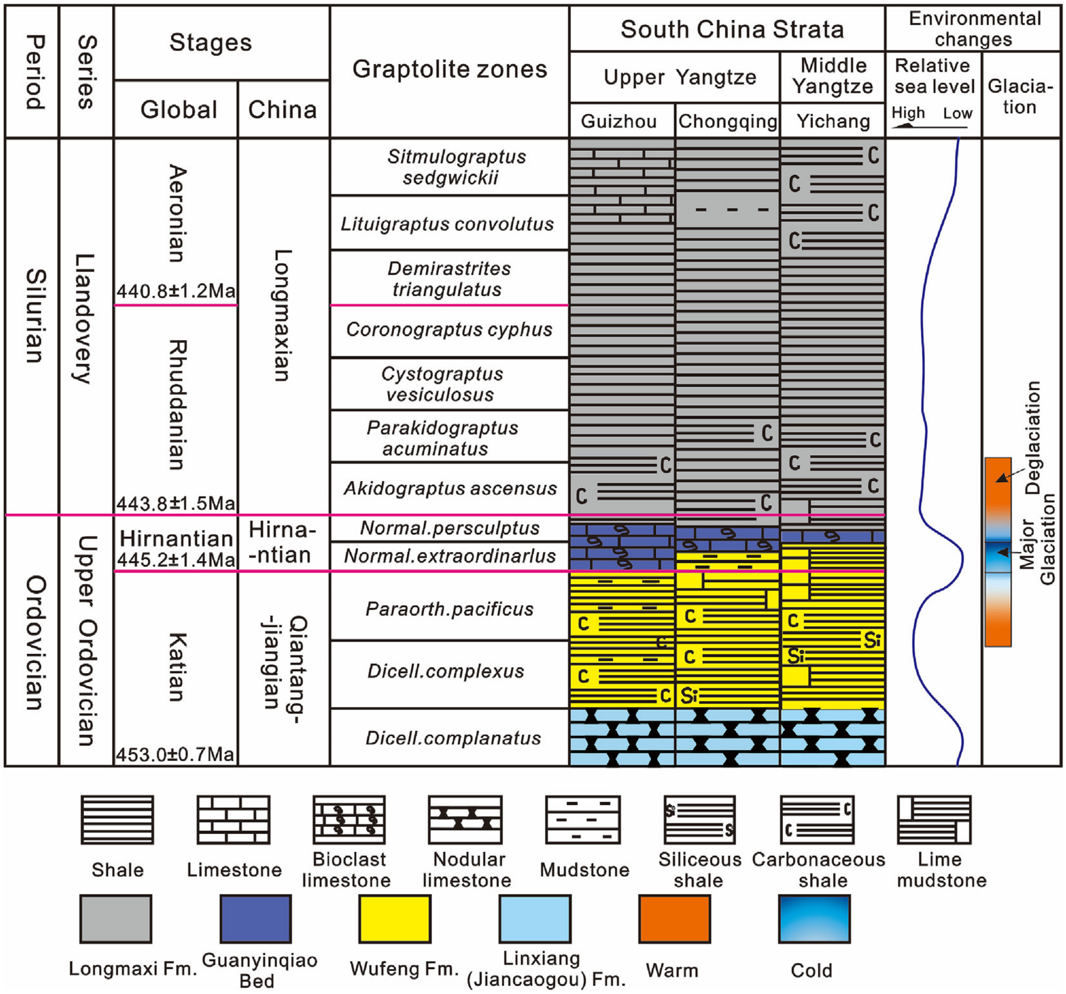

Fig. 2. Stratigraphic structure and lithology combination in the Ordovician-Silurian transition period, including the Late Ordovician Katian stage and Hirnantian stage to the Early Silurian Rhuddanian stage and Aeronian. Stratigraphic units include the Upper Ordovician Wufeng Formation, Guanyinqiao bed and the Silurian Longmaxi Formation. The age of the global stage isbased on International Chronostratigraphic Chart 2018. The age of the Chinese strata and graptolite biozones are referred by Chen et al. (2000), 2005; Fan et al. (2011); Chen et al. (2014); and Shen et al. (2019). The environment changes are referred by Wang et al. (2019a) , (2019b) .

facies, shallow sea shelf facies and confined shallow sea deep-water shelf facies (Fig. 1B). In the Upper Yangtze area, the lithologic association was mainly composed of grayish-black lamellar carbonaceous shale, while in the Middle Yangtze area, the rocks were mainly siliceous shale (Fig. 2). Generally, the shales contained some volcanic ash beds and pyrite nodules, and abundant protists fossils, such as graptolites and radiolarians, were found. The general thickness of the black shale was approximately 6–10 m, and the maximum thickness could reach 50 m (Sun et al., 2018).

In the depositional period of the Guanyinqiao bed, it was bearing the well-known Hirnantia Fauna, a cool-water shelly fauna that was widespread during the Hirnantia glaciation and disappeared abruptly when the glacial period ended (Lu et al., 2019). Because of glacial retreat and Caledonian movement, the paleo-uplift area in SC expanded, the basin area decreased and the depth of the water became shallow (Fig. 1C). The lithologic associations were dominated by limestone, argillaceous limestone and limey mudstone, and the sedimentary facies included tidal flat facies, shallow-water shelf facies and confined shallow-water shelf facies. The scope of the deep-water continental shelf was relatively small and limited to the Yibin-Luzhou area. Compared with that in the late Katian stage, the range of submarine highs was greatly expanded. The overall thickness of the Guanyinqiao bed was small. From the Upper Yangtze to the Middle Yangtze, the thickness of the Guanyinqiao bed showed a trend of gradual thinning. In most areas, the thickness was 0.2–1 m, and in some areas, it reached 10 m (Fig. 2).

In the Rhuddanian stage of the early Silurian (the first member of the Longmaxi Fm.), under the influence of glacier melting due to global warming, the sea rose dramatically, and the underwater uplifts were submerged. In this stage, the most typical feature was the rapid and extensive deposition of graptolite shale, and its lithology was dominated by carbonaceous calcareous shale and carbonaceous siliceous shale, which became the main gas-producing horizon of the Fuling shale gas field in China (Wu et al., 2018). The area with relatively thick shale was distributed in three hydrocarbon-rich depressions, namely, Yanjin-luzhou, Wulong-pengshui and Shizhu-wuxi, with thicknesses of 30–40 m. The centers of these depressions became connected to form a rich hydrocarbon zone to the northeast (Fig. 1D).

3. Samples and methods

3.1. Samples

Three outcrops in SC were investigated in detail (Fig. 1), and some ash samples from the Upper Ordovician Wufeng Fm. and lower Silurian Longmaxi Fm. were collected to carry out precise zircon U–Pb dating.

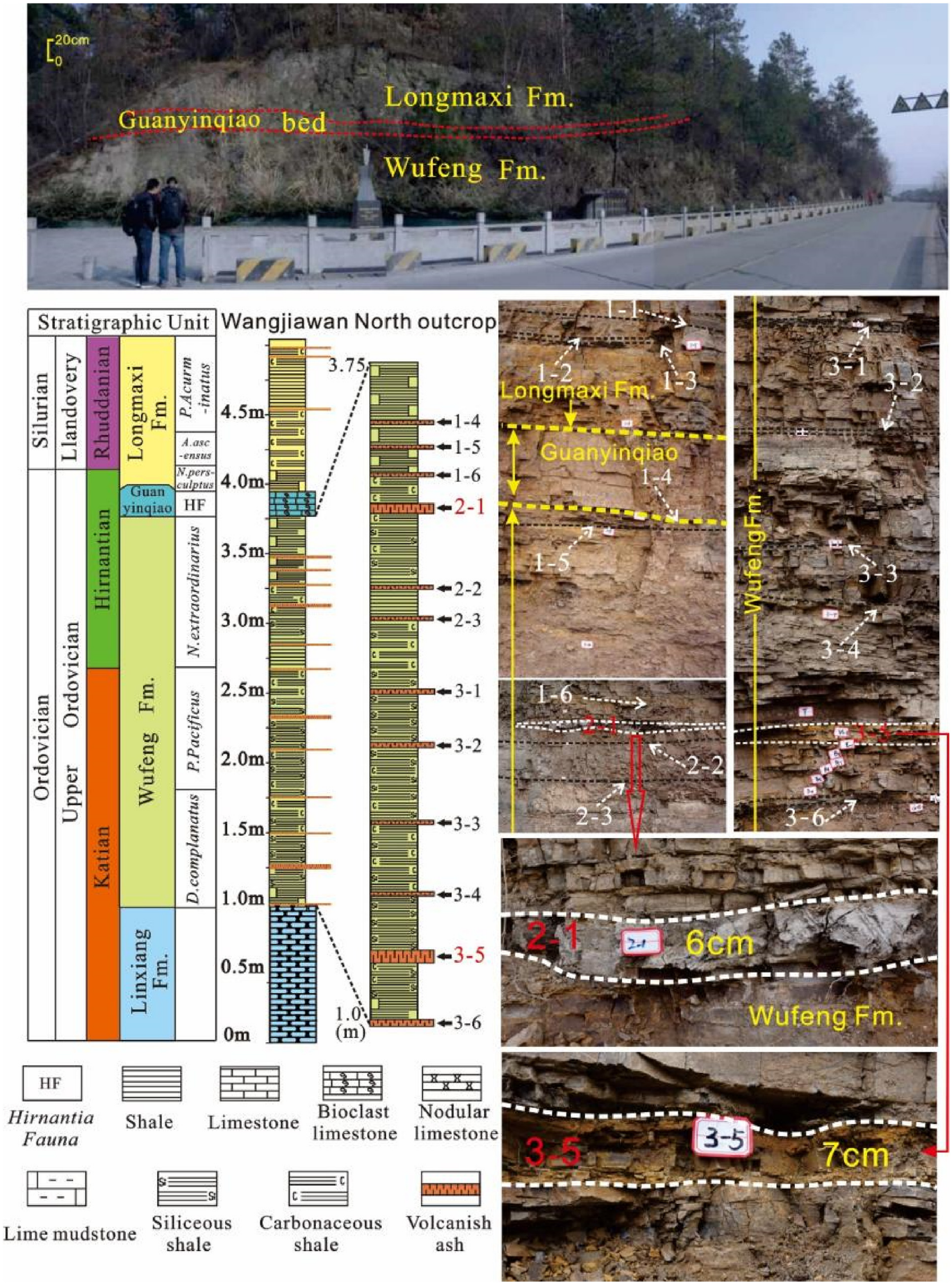

Fig. 3. Volcanic ash beds in the Wangjiawan North outcrop, Yichang County, Hubei Province. There are 15 layers of volcanic ash beds in this outcrop, including 12 layers of volcanic ash in the Wufeng Fm. and 3 layers of volcanic ash in the lower part of the Longmaxi Fm. We collected two samples from the No. 3–5 volcanic ash beds and the No. 2-1 volcanic ash beds for zircon U–Pb dating. The graptolite biozone isbased on Hu et al. (2008).

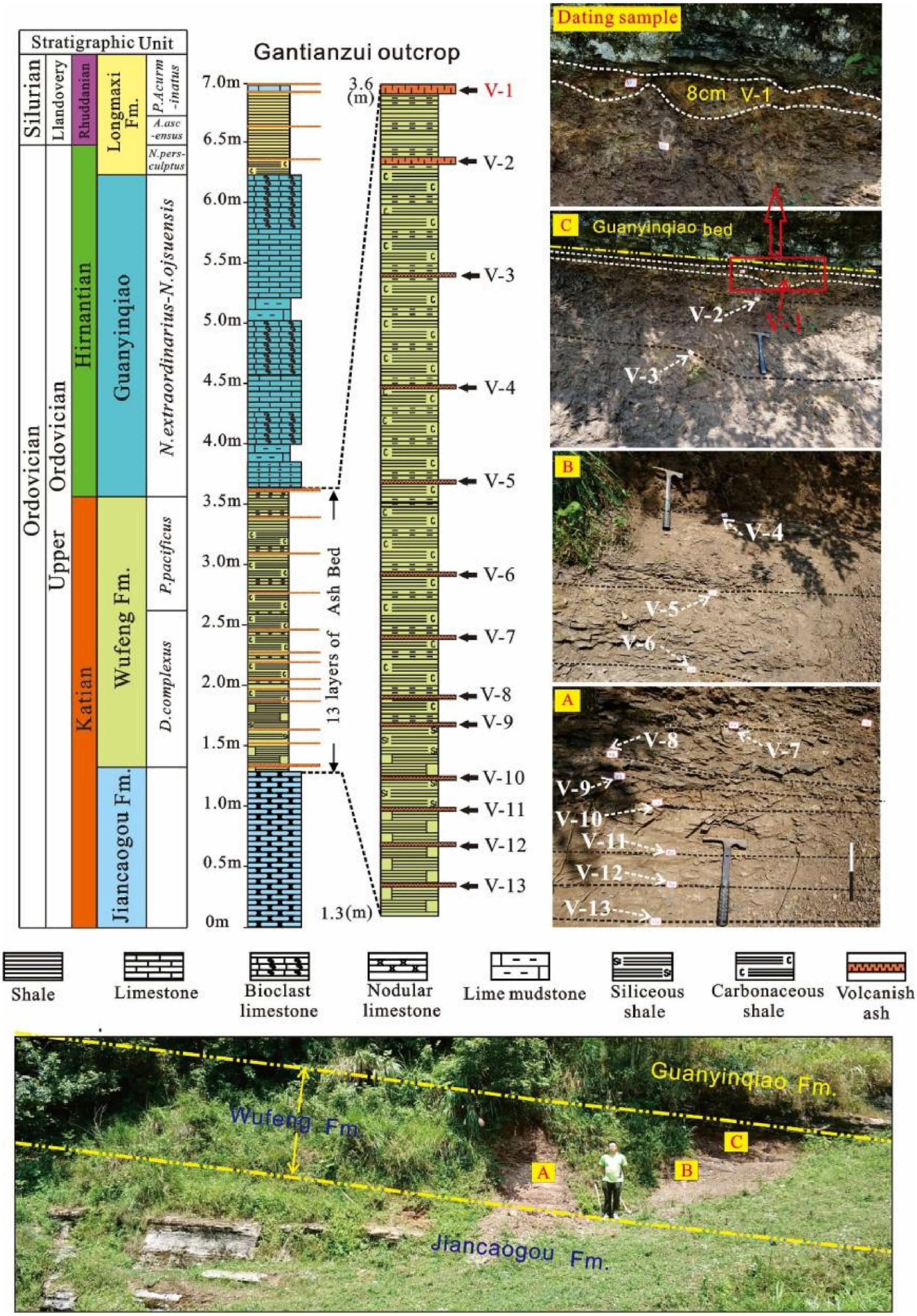

Fig. 4. Volcanic ash beds of the Ordovician Wufeng Fm. in the Gantianzui outcrop, Tongzi County, Guizhou Province. Thirteen layers of volcanic ash beds are identified in this area, and we collected a V-1 sample for zircon U–Pb dating. The graptolite biozone is based on Yan et al., 2015a,2015b.

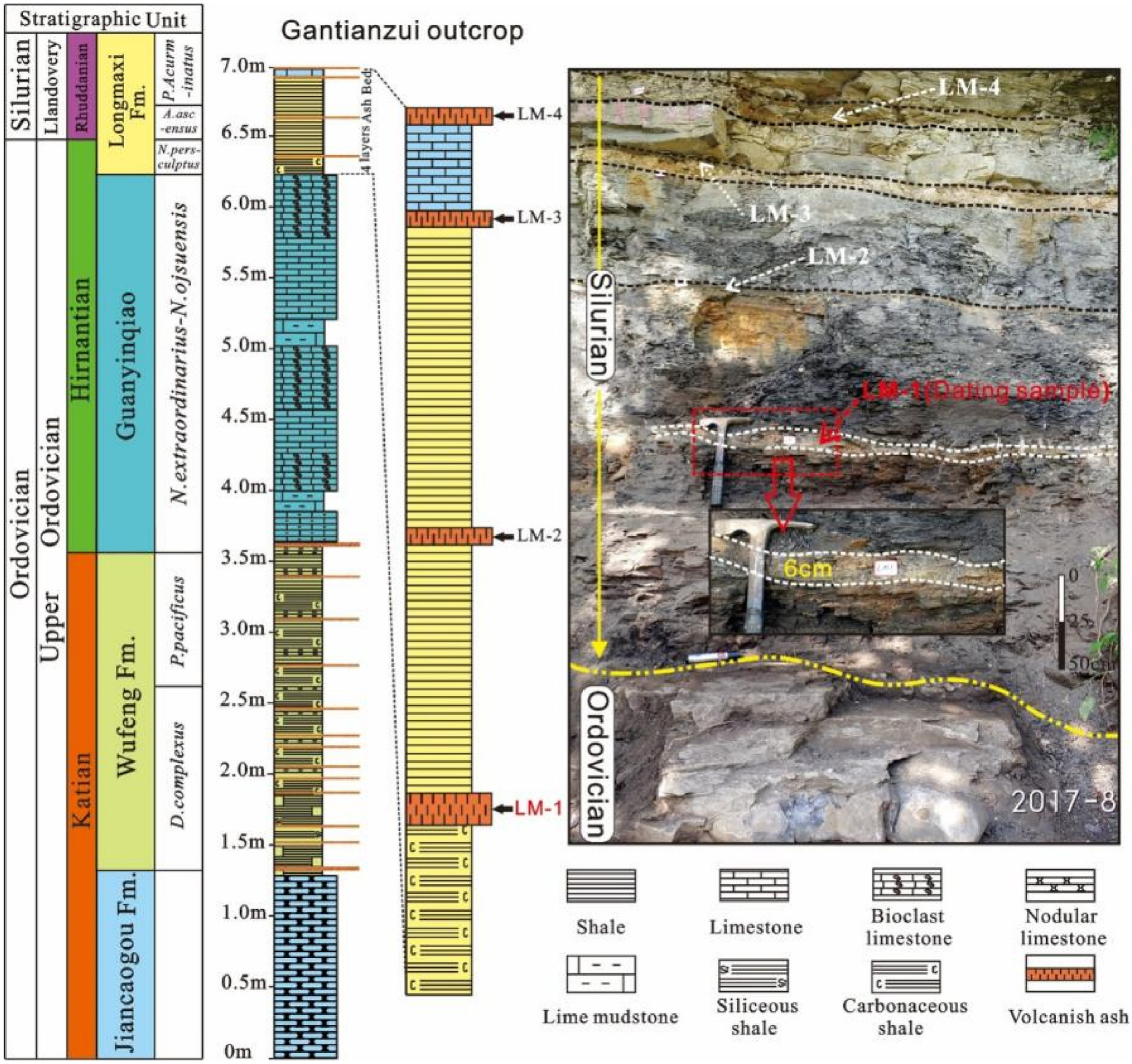

Fig. 5. Volcanic ash beds of the lower Silurian Longmaxi Fm. in the Gantianzui outcrop, Tongzi County, Guizhou Province. Four layers of volcanic ash beds are identified in this area, and we collected an LM-1 sample for zircon U–Pb dating. The graptolite biozone is based on Yan et al., 2015a,2015b.

3.1.1. Wangjiawan North outcrop

Wangjiawan North (N30°58′56″, E111°25′10″) is located in Yichang County, Hubei Province and represents a global boundary stratotype section and point (GSSP) for the base of the Hirnantian stage (the uppermost of the Ordovician system), because of its advantageous features, such as continuous sedimentation and biozonation, complete exposures, abundant and well-preserved graptolites and shelly fossils, favorable facies and widespread correlation potential (Chen et al., 2006). The Upper Ordovician Lingxiang Fm. (nodular limestone), Wufeng Fm. (siliceous shale and carbonaceous shale), Guanyingqiao bed (bioclast limestone), and lower Silurian Longmaxi Fm. (shale and carbonaceous shale) are continuously distributed in the vertical direction (Fig. 3).

Fifteen layers of volcanic ash beds are identified in this area, including 12 layers of volcanic ash in the Wufeng and 3 layers of volcanic ash in the lower part of the Longmaxi Formation. The volcanic ash beds in the Longmaxi Fm. are thinner, with the thickest at only 0.8–1 cm; and the volcanic ash beds in the upper and lower parts of the Wufeng Fm. are thicker, with the thickest volcanic ash bed at 5–8 cm. Due to the degree of weathering, some ash beds appear yellow, some appear gray, and some are gray black. We collected two examples from the No. 3–5 and No. 2-1 volcanic ash beds (Fig. 3). The No. 3–5 volcanic ash beds are at the bottom of the Wufeng Fm. and 7 cm thick, and the measurement of their ages can approximately determine the beginning time of the Wufeng Fm. The No. 2-1 volcanic ash beds are at the top of the Wufeng Fm. and 6 cm thick, and the measurement of their ages can determine the end time of the Wufeng Fm. and the beginning time of the Guanyinqiao bed (Fig. 3).

3.1.2. Gantianzui outcrop

Gantianzui (N28°3′46″, E106°51′36″) is located in Tongzi County, Guizhou Province, approximately 10 km from Zunyi City. The exposed strata here include the Ordovician Jiancaogou Fm., Wufeng Fm., Guanyinqiao bed and the Silurian Longmaxi Fm. Seventeen layers of volcanic ash beds have been identified in this area, including 13 layers of volcanic ash in the Ordovician Wufeng Fm. and 4 layers of volcanic

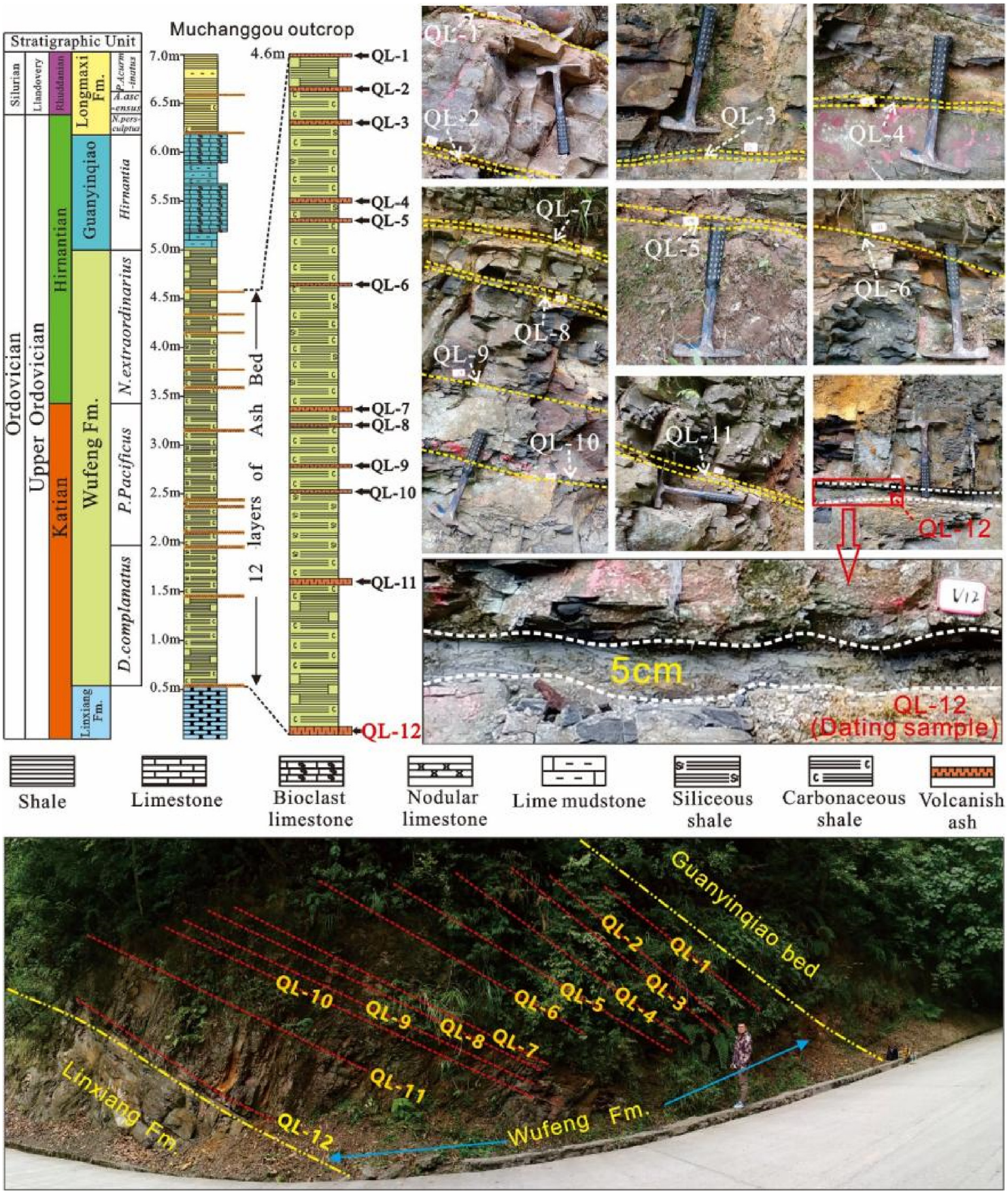

Fig. 6. Volcanic ash beds of the Wufeng Fm. in the Muchanggou outcrop, Shizhu County, Chongqing City. There are 12 layers of volcanic ash beds in this outcrop. We collected one sample from the No. QL-12 volcanic ash bed for zircon U–Pb dating. The graptolite biozone is based on by Wang et al. (2019a) ,(2019b).

ash in the lower segment of the Silurian Longmaxi Fm. These layers are well developed horizontally.

The thicknesses of the volcanic ash beds in the Ordovician Wufeng Fm. are different. The V-1, V-2 and V-3 volcanic ash beds are thicker, with V-1 the thickest at 5–8 cm, and it is also a sampling layer. V-2 and V-3 are 3 cm and 5 cm, respectively. The other ash beds are thinner, with the thinnest only 0.1 cm (Fig. 4).

In the Silurian Longmaxi Fm., we identified four volcanic ash beds, with the thickest reaching 10 cm and the thinnest reaching 3–5 cm. The bottom of the Longmaxi Fm. is gray-black thinly layered bioclastic limestone, and the top of the Guanyinqiao bed is bioclastic limestone. At the boundary between the Longmaxi Fm. and Guanyinqiao bed, there is a volcanic ash bed (LM-1) 6 cm in thickness, and it is the sampling layer for zircon U–Pb dating (Fig. 5).

3.1.3. Muchanggou outcrop

Muchanggou (N29°52′42.19″, E108°16′58.72″) is located in Shizhu County, Chongqing City, which is on the Shizhu syncline belt. The exposed strata here are the Ordovician Linxiang Fm., Wufeng Fm., Guanyinqiao bed and the Silurian Longmaxi Fm. Fourteen volcanic ash

Table 1
U–Pb zircon ages using the LA-ICP-MS method from volcanic ash beds 3–5 at the bottom of the Wufeng Formation in the Wangjiawan North outcrop.

Number	^{232}Th(ppm)	^{238}U(ppm)	U/Th	^{207}Pb/^{206}Pb	1δ	^{207}Pb/^{235}U	1δ	^{206}Pb/^{238}U	1δ	^{206}Pb/^{238}U (Ma)	1δ
1	910.0082	635.5618	0.8326479	0.058869654	0.001666766	0.579842482	0.01468175	0.071785475	0.001791905	446.9036302	10.78038073
2	943.738	798.0064	0.864353672	0.058956551	0.001488881	0.588108707	0.015895599	0.071538805	0.001412164	445.4198303	8.499030808
3	388.9934	460.8728	1.199246438	0.049631229	0.001660306	0.4939647	0.017447541	0.071480463	0.001590841	445.0688333	9.574094097
4	422.6495	473.0078	1.139317871	0.056080501	0.001592716	0.557671194	0.015897393	0.071701755	0.001645233	446.4000694	9.899206178
5	623.0358	799.1662	1.304381352	0.056421546	0.001384984	0.561270215	0.014480942	0.071012332	0.001371005	442.2517686	8.255523218
6	239.4767	307.4435	1.282845105	0.057671919	0.002083348	0.570483654	0.021769183	0.070983771	0.00181237	442.0798613	10.9115401
7	382.9931	463.5824	1.258031182	0.057638389	0.001583804	0.57673973	0.0165279	0.07166782	0.001439648	446.1959418	8.663280806
8	309.9965	393.5901	1.273446684	0.054280436	0.00140056	0.544934941	0.01606324	0.071759991	0.001484087	446.7503525	8.929735966
9	415.8502	490.8258	1.16786229	0.056376353	0.001339688	0.559987682	0.012840426	0.071663734	0.001298092	446.171363	7.812174585
10	426.2864	504.1457	1.1635078	0.057313296	0.001461262	0.568261884	0.015164367	0.071771248	0.00155735	446.8180608	9.370148352
11	444.9228	517.4594	1.131561231	0.059574451	0.001404088	0.592948959	0.016717409	0.071772509	0.001482364	446.8256445	8.91927516
12	285.1984	533.7064	1.901757331	0.06225149	0.001614061	0.609882938	0.017068076	0.071640945	0.001934606	446.0342742	11.64004066
13	711.7492	550.6862	0.762894465	0.055385325	0.001229624	0.551269371	0.0140006	0.071863709	0.001496068	447.3741661	9.000913222
14	273.4102	338.3393	1.193363677	0.054020647	0.001458889	0.540113519	0.015928097	0.07218096	0.001638899	449.2819003	9.856754296
15	420.6527	474.7175	1.093029984	0.057166041	0.001516549	0.57445994	0.017148156	0.072270757	0.001596996	449.8217744	9.604097657
16	515.2739	519.7454	0.973300126	0.051577422	0.001335858	0.511661177	0.013151683	0.071662776	0.001606187	446.1655972	9.664760624
17	186.7549	308.0374	1.584638472	0.054842578	0.001487048	0.544980541	0.016273056	0.071801167	0.001913438	446.9980131	11.51102097
18	390.7151	440.4174	1.073261193	0.061816999	0.00225988	0.619449768	0.024658376	0.071688681	0.001583486	446.3214246	9.528019617
19	172.6998	249.3946	1.443733716	0.055036329	0.001795495	0.549474598	0.019859931	0.071741729	0.001827385	446.6405129	10.9941745
20	135.3362	206.5181	1.445759414	0.060685135	0.003130378	0.596208781	0.031663113	0.070643698	0.001711415	440.0325848	10.3072796
21	148.6533	206.3877	1.428563111	0.054932768	0.002109329	0.546585103	0.023035429	0.071727064	0.001760877	446.5523031	10.59438221
22	238.962	333.3741	1.427279814	0.060596031	0.00179911	0.609430457	0.020857329	0.071757703	0.00150928	446.7365898	9.081231801
23	149.761	290.9321	1.973672297	0.054198407	0.001459827	0.540541708	0.015264605	0.071855054	0.001476358	447.3221109	8.882487585
24	464.9081	471.0078	0.998453845	0.053150817	0.00127473	0.523255046	0.012556646	0.071018372	0.001282309	442.2881248	7.721856808
25	459.1686	483.1575	1.029570373	0.05774902	0.001455647	0.570718547	0.015843516	0.071455976	0.001511243	444.921509	9.095564617
26	280.0427	391.1772	1.349226392	0.055399609	0.001590971	0.545579251	0.017025588	0.071520177	0.001692772	445.3077582	10.18679151
27	121.5122	206.8734	1.646761364	0.055631678	0.002058839	0.54851714	0.02150269	0.071297889	0.001529355	443.9703091	9.2058433
28	211.5871	470.4673	2.124283921	0.057596921	0.001365699	0.562311173	0.013677558	0.070704113	0.001359254	440.3963336	8.187148158
29	412.3298	489.4675	1.136974436	0.052977662	0.001272251	0.5213368	0.012764928	0.071239678	0.001484063	443.6200164	8.933880293
30	358.3786	437.6345	1.168606825	0.052256627	0.001572923	0.51434818	0.015152068	0.071648811	0.001759716	446.0815935	10.58816281
31	239.7469	334.365	1.356536368	0.055396812	0.001726578	0.547718252	0.017598295	0.071868097	0.001808145	447.4005529	10.8772018
32	337.3991	339.1675	0.920612949	0.057303998	0.001566237	0.562834066	0.015759128	0.070663525	0.001541829	440.1519613	9.286321741

Table 2
U–Pb zircon ages using the LA-ICP-MS method from volcanic ash beds 2-1 at the top of the Wufeng Formation in the Wangjiawan Northoutcrop.

Number	^{232}Th(ppm)	^{238}U(ppm)	U/Th	^{207}Pb/^{206}Pb	1δ	^{207}Pb/^{235}U	1δ	^{206}Pb/^{238}U	1δ	^{206}Pb/^{238}U (Ma)	1δ
1	388.7348	369.1626	1.058192927	0.052303604	0.000750538	0.51524053	0.007885379	0.07145442	0.00072297	444.912153	4.35638342
2	205.5381	269.8585	1.40701164	0.057971697	0.001314607	0.57093135	0.015096488	0.07138845	0.001020565	444.515202	6.14530635
3	310.8956	406.1908	1.398464593	0.052944233	0.001137121	0.52214197	0.012343536	0.07143748	0.000832718	444.810238	5.01589058
4	528.9005	575.7974	1.188889799	0.055555917	0.00077974	0.5455846	0.008802838	0.07124995	0.000907859	443.681835	5.46843717
5	453.9878	653.2804	1.5357031	0.056137556	0.0007036	0.55408163	0.009546537	0.07151108	0.000957396	445.253027	5.76489409
6	283.2657	364.6543	1.387800892	0.061495519	0.001549969	0.60172276	0.016022875	0.07151709	0.001673159	445.289193	10.0688604
7	240.5662	322.8883	1.433187343	0.052193863	0.001060656	0.51128827	0.012013858	0.07104378	0.001050153	442.441043	6.32518881
8	243.938	273.1709	1.201621064	0.058233296	0.001139042	0.57476911	0.01274534	0.07153977	0.000903958	445.425617	5.44355595
9	476.5172	487.3158	1.154557112	0.057178266	0.001005229	0.56440271	0.011667829	0.07151694	0.001000427	445.288297	6.02352466
10	266.9173	379.3144	1.510387699	0.059390078	0.001006417	0.58423933	0.009826302	0.07132389	0.000857383	444.126759	5.16465466
11	207.282	229.7064	1.183190891	0.059733915	0.001281142	0.58755418	0.014381026	0.07107448	0.000931129	442.625822	5.60922544
12	496.4451	450.9495	0.97288996	0.061213106	0.001089328	0.60003325	0.010667232	0.07107834	0.000839211	442.649048	5.05654729
13	220.5213	209.1992	1.006835263	0.057961614	0.001103927	0.56992043	0.011757827	0.07131552	0.000858602	444.076414	5.17201899
14	443.486	665.0581	1.636299505	0.061612028	0.001690407	0.60494817	0.016583036	0.07123622	0.000674676	443.599227	4.06707796
15	343.5161	383.8938	1.226680088	0.056920417	0.001073329	0.56103884	0.010998383	0.07150376	0.000765745	445.209013	4.61316545
16	528.0723	726.0844	1.457665514	0.052190468	0.000673716	0.51387516	0.007346456	0.07139545	0.000767411	444.557314	4.62362655
17	238.7779	368.5358	1.639463989	0.051108675	0.000938765	0.50232816	0.0089829	0.07140063	0.000811932	444.5885	4.89113577
18	271.3265	395.5647	1.54856813	0.05213424	0.000879737	0.51142118	0.008837501	0.07110474	0.000824713	442.807951	4.96926856
19	336.015	280.0685	0.895557397	0.056864901	0.00093443	0.56116512	0.010556856	0.07146621	0.00095819	444.983053	5.76989756
20	638.7229	828.8387	1.374907175	0.059787605	0.001077328	0.586242	0.010165127	0.0712311	0.000896312	443.568403	5.39910766
21	646.3785	630.7511	1.031767466	0.057172735	0.00066869	0.5619921	0.008019173	0.0713541	0.000902971	444.308541	5.43853798
22	209.5494	338.957	1.700131316	0.051303358	0.000773964	0.50775719	0.00766806	0.07186726	0.000775807	447.395535	4.67210266

beds are identified in this outcrop, including 12 layers of volcanic ash in the Ordovician Wufeng Fm. and 2 layers of volcanic ash in the lower segment of the Silurian Longmaxi Fm. Overall, the degree of weathering of volcanic ash is relatively weak, and the ash is gray or grayish-yellow in color (Fig. 5). Their thicknesses are stable, and the horizontal continuity is good.

In the boundary between the Linxiang Fm. (nodular limestone) and Wufeng Fm. (calcareous shale), there is a gray volcanic ash bed (QL-12) with a thickness of 5 cm, which is the thickest volcanic ash bed in the Wufeng Fm. Thus, we collected volcanic ash from QL-12 for the age determination (Fig. 6).

3.2. Methods

The volcanic ash beds in three outcrops are loose and brittle due to long-term weathering, making them easy to collect. Each collected sample is at least 3 kg. In the lab, these samples were further crushed and heavy minerals were separated. Under a microscope, transparent zircon grains with intact crystal shapes were picked. Then, these zircons were fixed onto thin sections for microscopic examination. In order to get a meaningful geological age, one must pay attention to the cathodoluminescence (CL) images of zircons to examine zircons' internal structures and genetic processes before dating (Zhu et al., 2013).

We used two methods for zircon U–Pb dating. Samples 3–5, 2-1, V-1, LM-1, and QL-12 were analyzed by the LA-ICP-MS method, and sample 2-1was also analyzed by the SHRIMPII method to compare the reliability of the data from the LA-ICP-MS method. In the course of data processing, Grains interpreted to be xenocrysts, based on their Precambrian ages, were not used in the calculation of ages from samples dated here.

3.2.1. LA-ICP-MS method

The zircon U–Pb precise dating was carried out in the Hubei Geological ResearchLaboratory using an Agilent 7700X ICP-MS. The diameter of the laser spot was 32 μm. International standards 91500, GJ-1 and Plešovice were acted as external standards (Wiedenbeck et al., 1995) and measured every 5 samples to ensure the stable working condition of the instrument. The Pb isotope ratios, U–Pb surface ages and trace element contents of zircon were calculated with ICP-MS DataCal (3.5) software and U–Pb concordia plots were drafted by Isoplot (3.23) (Ludwig, 2012).

3.2.2. SHRIMP method

The other U–Pb dating method was used the SHRIMP II ion microprobe at the Beijing SHRIMP Center, Chinese Academy of Geological Sciences (CAGS). The analytical procedure for zircon dating was similar to that described by Williams (1998). The intensity of the primary O^{2-} ion beam was 4–6 nA. The primary beam size was ~30 μm, and each analytical site was rastered for 2–3 min prior to analysis. Five scans through the relevant mass stations were performed for each analysis. The standards used were SL13 (U = 238 ppm) and TEMORA (^{206}Pb/^{238}U age = 417 Ma) (Williams, 1998; Black et al., 2003; Wan et al., 2012). The measured ^{204}Pb was applied for common lead correction, and data processing was carried out using the SQUID and ISOPLOT programs (Ludwig, 2002). Uncertainties for individual analyses are quoted at the 1σ confidence level, whereas errors for weighted mean ages are quoted at the 95% confidence level.

4. Results

4.1. LA-ICP-MS zircon U–Pb dates

Samples 2-1 and 3–5 are from the Wangjiawan North outcrop. After removing data with less than 90% concordance, 32 points in the 3–5 example and 22 points in the 2-1 example can be used for analysis (Tables 1 and 2). Fig. 7A shows that the ^{206}Pb/^{238}U age of 3–5 is between 430 Ma and 458 Ma, and the mean age is 446.6 ± 1.3 Ma (MSWD = 0.018, n = 32). Fig. 7B shows that the ^{206}Pb/^{238}U age of 2-1 is between 435 Ma and 450 Ma, and the mean age is 445.4 ± 1.2 Ma (MSWD = 0.046, n = 22).

Samples V-1 and LM-1 are from the Gantianzui outcrop. Every sample contains 300 zircons, 80 of which were selected for LA-ICP-MS zircon U–Pb dating analysis. After removing data with less than 90% concordance, 22 points in the V-1 sample and 29 points in the LM-1 sample can be used for analysis (Tables 3 and 4). The final results are shown in Figs. 7C and 8A.

Fig. 7C shows that the^{206}Pb/^{238}U age of V-1is between 438 Ma and 455 Ma, and the mean ^{206}Pb/^{238}U age is 445.6 ± 0.9 Ma (MSWD = 0.018, n = 22). Fig. 8A shows that the ^{206}Pb/^{238}U age of LM-1 is between 430 Ma and 456 Ma, and the mean ^{206}Pb/^{238}U age is 444.4 ± 0.9 Ma (MSWD = 0.024, n = 29).

Sample QL-12 is from the Muchanggou outcrop. After removing data with less than 90% concordance, 35 points can be used for analysis (Table 5). The final result is shown in Fig. 8B. The ^{206}Pb/^{238}U age of

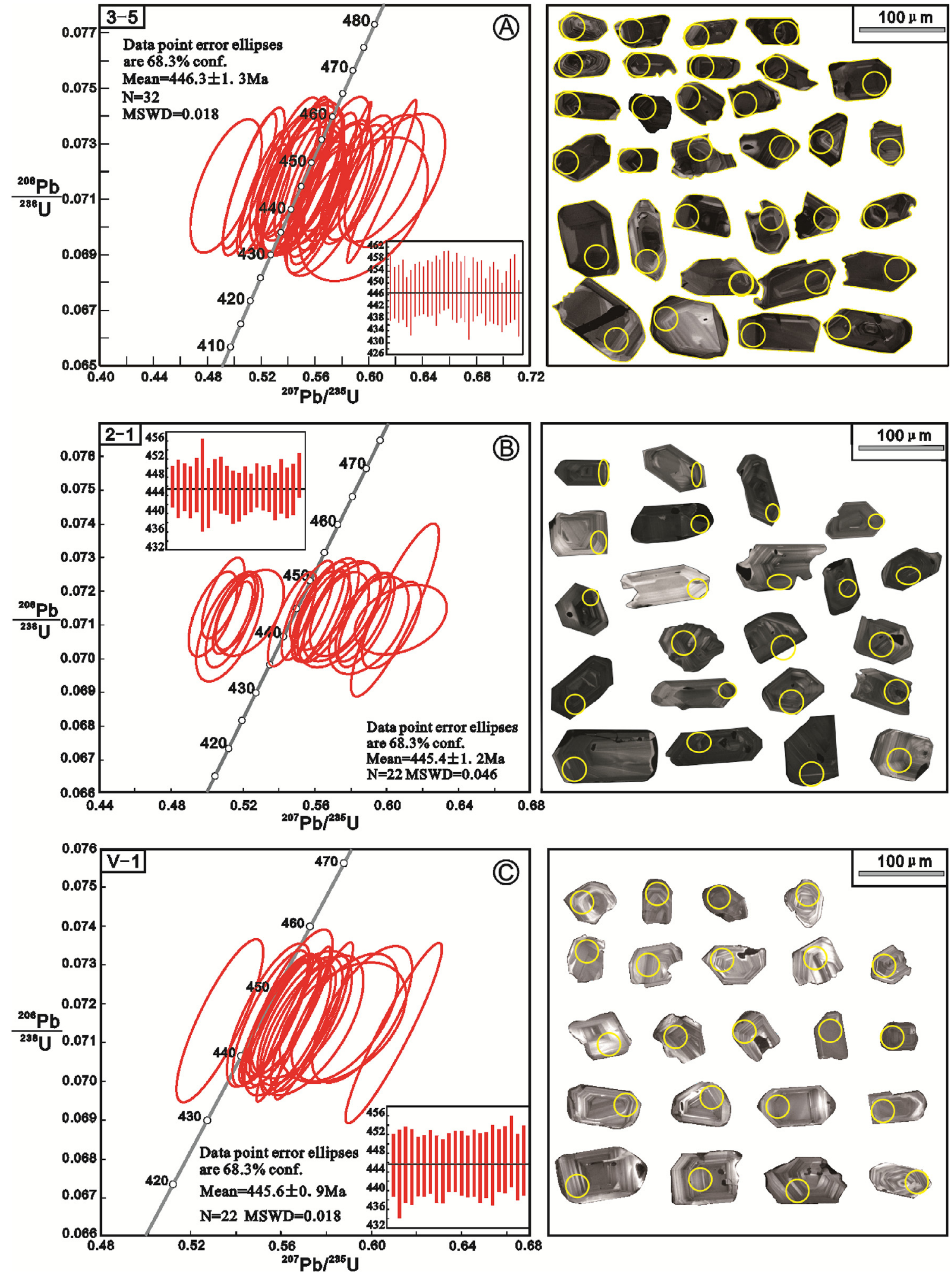

Fig. 7. (A) U–Pb concordia plots (left) and cathodoluminescence (CL) images of selected zircons and dating locations (right) for zircons from volcanic ash beds 3–5 at the bottom of the Wufeng Formation in the Wangjiawan outcrop. (B) U–Pb concordia plots (left) and cathodoluminescence (CL) images of selected zircons and dating locations (right) for zircons from volcanic ash beds 2-1 at the top of the Wufeng Formation in the Wangjiawan outcrop. (C) U–Pb concordia plots (left) and cathodoluminescence (CL) images of selected zircons and dating locations (right) for zircons from volcanic ash bed V-1 at the top of the Wufeng Formation in the Gantianzui outcrop.

Table 3
U–Pb zircon ages using the LA-ICP-MS method from volcanic ash beds V-1 at the top of the Wufeng Formation in the Gantianzui outcrop.

Number	^{232}Th(ppm)	^{238}U(ppm)	U/Th	^{207}Pb/^{206}Pb	1δ	^{207}Pb/^{235}U	1δ	^{206}Pb/^{238}U	1δ	^{206}Pb/^{238}U (Ma)	1δ
1	362.4709	412.9061	0.96918767	0.057445936	0.00098511	0.568831863	0.01241	0.071538681	0.00108	445.419083	6.5139668
2	209.5196	264.6331	1.128984076	0.063588455	0.001842813	0.617738255	0.01414	0.071237435	0.00153	443.606522	9.237116
3	260.3892	410.3571	1.325489934	0.058222117	0.001022991	0.574889099	0.01137	0.071554977	0.00132	445.517119	7.9546851
4	257.8121	320.2708	1.067203424	0.057387491	0.00090251	0.565804117	0.01078	0.071477364	0.00131	445.050188	7.8681905
5	140.8808	303.2475	1.795609048	0.059674546	0.001881959	0.58768828	0.01863	0.071498655	0.00102	445.178277	6.1115181
6	210.9061	348.6025	1.381163081	0.056253529	0.000739657	0.556419521	0.00966	0.071509188	0.00105	445.241651	6.338088
7	296.4055	382.2254	1.057167038	0.059734581	0.001646957	0.588696606	0.01543	0.071648194	0.00109	446.077885	6.5424011
8	146.6904	250.3268	1.419570923	0.057221054	0.001042113	0.563231753	0.0128	0.071392983	0.00116	444.542498	6.9969701
9	162.3065	282.3624	1.460030739	0.058101662	0.001134366	0.567761515	0.01108	0.071314885	0.0011	444.072576	6.6196618
10	303.2351	464.3247	1.286179443	0.056618319	0.000763521	0.558639999	0.00935	0.071630223	0.001	445.969777	6.0087751
11	558.6341	743.3678	1.113614729	0.057282605	0.000789126	0.56551945	0.00957	0.071674706	0.00105	446.23736	6.3064733
12	687.2454	802.3368	0.983814447	0.056697488	0.000804101	0.559711727	0.00967	0.071607229	0.00112	445.831456	6.7192338
13	368.9074	482.883	1.073955388	0.056814234	0.000817892	0.561603379	0.01014	0.071495491	0.00105	445.159244	6.3493158
14	151.1422	264.4165	1.464620282	0.056194783	0.000911798	0.555579122	0.01115	0.07161359	0.00116	445.869721	6.9776741
15	158.6695	271.0683	1.428349384	0.058143527	0.001228962	0.573980442	0.01503	0.071428928	0.0012	444.758773	7.2197377
16	167.4268	334.7759	1.655972265	0.056798196	0.000972147	0.560266401	0.0114	0.071547174	0.00114	445.470178	6.8599747
17	198.8716	264.6539	1.123457045	0.053965097	0.000977994	0.533245185	0.01251	0.071548365	0.0014	445.477341	8.3961682
18	124.5064	205.7683	1.410304522	0.057332651	0.001317057	0.569396345	0.01457	0.07170302	0.00108	446.407676	6.497093
19	124.6486	264.6994	1.764226046	0.059970791	0.00121474	0.596309946	0.01458	0.071738262	0.00116	446.619659	6.9874124
20	355.0883	411.8068	0.965807704	0.056794373	0.001039721	0.564784068	0.01201	0.072028525	0.00124	448.365327	7.4644506
21	227.4336	322.5843	1.210630998	0.058319502	0.001239134	0.573051255	0.01121	0.071472571	0.00114	445.021351	6.875772
22	105.0064	210.1123	1.667235744	0.056007623	0.00108003	0.554623315	0.01221	0.071711292	0.00121	446.457435	7.3036021

Table 4
U–Pb zircon ages using the LA-ICP-MS method from volcanic ash beds LM-1 in the lower Longmaxi Formation in the Gantianzui outcrop.

Number	^{232}Th(ppm)	^{238}U(ppm)	U/Th	^{207}Pb/^{206}Pb	1δ	^{207}Pb/^{235}U	1δ	^{206}Pb/^{238}U	1δ	^{206}Pb/^{238}U (Ma)	1δ
1	123.3111	216.6672	1.478270895	0.055483188	0.00118	0.552362114	0.01501	0.071852999	0.001323873	447.3097546	7.965794384
2	112.6618	180.5334	1.380141206	0.061066523	0.00211	0.564138312	0.0174	0.068337196	0.001740872	426.1300085	10.50705108
3	238.067	414.4574	1.491693371	0.05635931	0.001	0.558801227	0.01471	0.071412445	0.00136652	444.6595977	8.225508712
4	116.9246	214.9398	1.587654836	0.058831998	0.00124	0.564490466	0.0144	0.069288047	0.001291755	431.8649524	7.791092877
5	260.077	562.612	1.90483588	0.055492232	0.00103	0.551044811	0.01227	0.071617711	0.001328063	445.8945136	7.992711171
6	189.7087	474.2144	2.175511911	0.059685912	0.00123	0.582963069	0.0127	0.07066633	0.00125393	440.1688522	7.553573059
7	143.9861	301.0558	1.77179387	0.057678334	0.00124	0.577626596	0.01539	0.0723924	0.001377159	450.5530401	8.282015789
8	149.7625	279.3745	1.586436745	0.05705302	0.00118	0.559577531	0.01398	0.070754211	0.001077621	440.6979557	6.492116683
9	142.0878	283.5403	1.716823527	0.058078671	0.00116	0.568598631	0.01378	0.070979345	0.001278262	442.053221	7.697788403
10	156.4563	354.9907	1.889897421	0.057158607	0.00112	0.560272911	0.01317	0.071251771	0.001361855	443.6927895	8.198661832
11	176.1051	419.9663	1.984364425	0.057534736	0.001	0.5649185	0.01269	0.071286248	0.001350992	443.9002579	8.133064987
12	61.77386	108.9693	1.506168035	0.054001171	0.00168	0.526180876	0.01768	0.071120182	0.001569846	442.9008845	9.450962361
13	124.1854	238.3228	1.614253719	0.058764732	0.00134	0.577897637	0.01681	0.071366697	0.00143502	444.3843402	8.637848025
14	214.365	430.971	1.697588271	0.0576973	0.00112	0.576130605	0.01492	0.07218409	0.001299626	449.3007137	7.817654514
15	139.4436	339.8942	2.072751247	0.058587128	0.00121	0.581246633	0.015	0.071922106	0.001440855	447.7253658	8.668503622
16	204.9039	296.8769	1.228231034	0.057550729	0.00117	0.567183299	0.01446	0.071197225	0.00113494	443.3645439	6.834207279
17	196.6072	378.7921	1.666358203	0.055482603	0.00096	0.544720733	0.01083	0.071250844	0.001275553	443.6872145	7.679570764
18	142.204	210.3616	1.263898752	0.056472977	0.0014	0.561544974	0.01816	0.071623507	0.001427825	445.9293763	8.592539569
19	186.3235	346.5939	1.580426762	0.053414328	0.00313	0.529936872	0.02469	0.071590675	0.00248254	445.7318734	14.93626266
20	289.4973	492.3146	1.436137549	0.055725438	0.00093	0.541128562	0.01394	0.070037817	0.001360583	436.3835011	8.200180088
21	110.8587	265.6288	2.003800773	0.054034842	0.00109	0.547911576	0.01536	0.073036807	0.001231354	454.4255666	7.401592704
22	62.65423	141.1756	1.883416667	0.056365971	0.00152	0.54989554	0.01469	0.071407815	0.00147619	444.6317398	8.885139449
23	220.2366	448.1118	1.704036124	0.055961979	0.00107	0.555288514	0.01565	0.071587654	0.001405458	445.7136967	8.458320912
24	230.2133	442.5823	1.610213882	0.059280826	0.00131	0.582725223	0.01564	0.071331254	0.00134889	444.1710711	8.120084307
25	268.6573	452.2784	1.427467569	0.057786064	0.00097	0.571252583	0.0135	0.071276639	0.001148695	443.8424379	6.916435298
26	193.964	402.568	1.733824332	0.059879505	0.00113	0.588406071	0.01543	0.071278555	0.001510226	443.8539651	9.090939296
27	69.59613	142.315	1.71021555	0.055287477	0.00131	0.543657491	0.01682	0.071291553	0.001531999	443.9321779	9.221801061
28	371.3099	648.9836	1.445326806	0.057749434	0.00124	0.564624781	0.01435	0.071197361	0.001258913	443.36536	7.579858825
29	115.5462	262.479	1.872683518	0.056730382	0.00118	0.553321368	0.01455	0.070683806	0.001239841	440.2740703	7.468668581

QL-12 is between 440 Ma and 458 Ma, and the mean ^{206}Pb/^{238}U age is 449.2 ± 1.3 Ma (MSWD = 0.066, n = 35).

4.2. SHRIMPII zircon U–Pb dates

Sample 2-1 is also selected to analyze the zircon age using the SHRIMPII method, and 21 points can be used for analysis (Table 6). In the course of data processing, the data on the Precambrian age were removed, and 21 data points remained. The final result is shown in Fig. 8C. The mean ^{206}Pb/^{238}U age of the 2-1 example is 445.1 ± 0.8 Ma (MSWD = 1.5, n = 21).

A comparison of the results for the 2-1 ash bed sample from the SHRIMPII method and the LA-ICP-MS method shows that the ^{206}Pb/^{238}U ages are statistically indistinguishable (445.1 ± 0.8 Ma; 445.4 ± 1.2 Ma). This consistency fully supports the reliability of the data obtained from the LA-ICP-MS method and shows that the ^{206}Pb/^{238}U age data obtained in this study for other ash beds are credible.

5. Discussion

5.1. Distribution of ash beds during the Late Ordovician period in SC

The three outcrops at Wangjiawan North, Gantianzui and

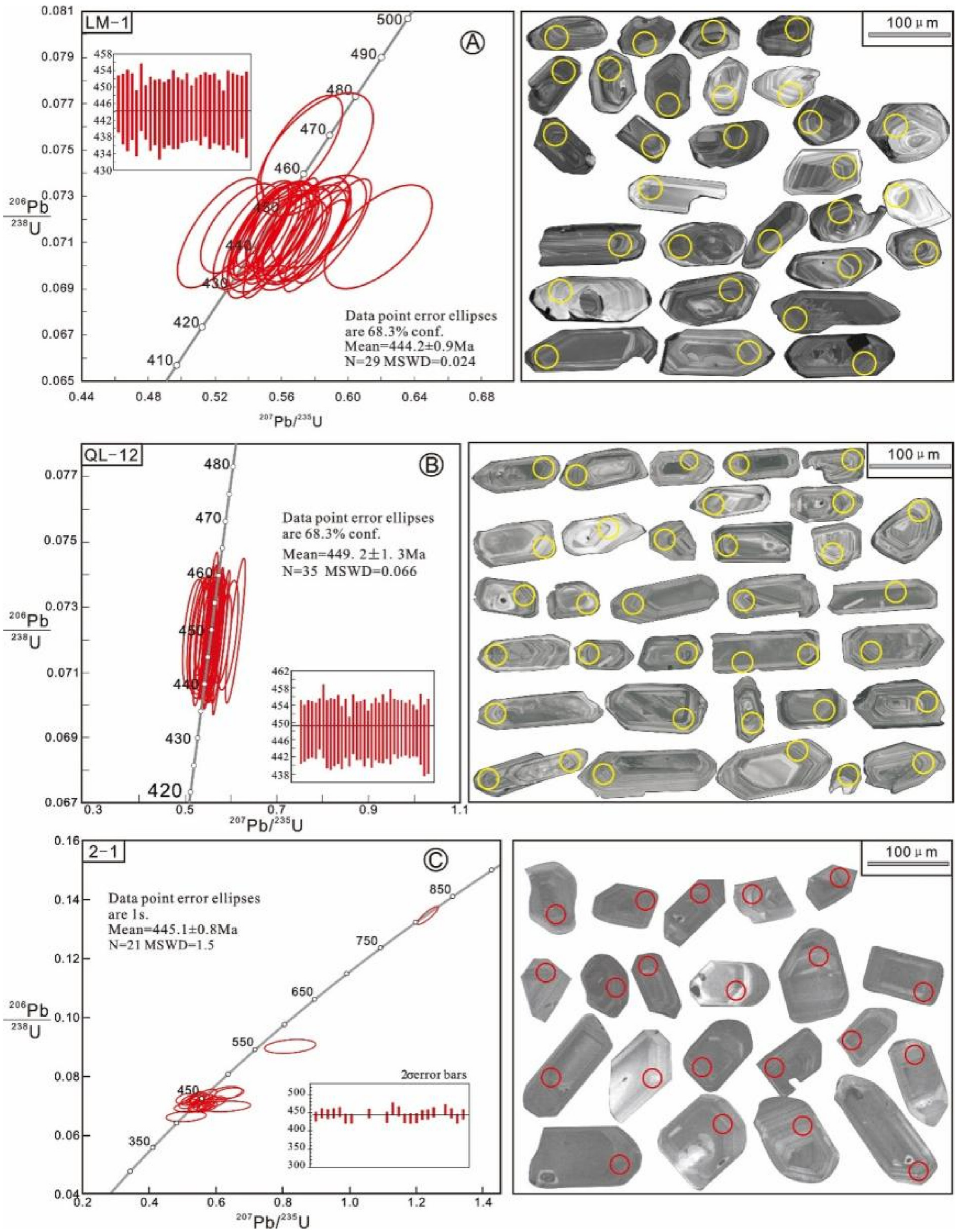

Fig. 8. (A) U–Pb concordia plots (left) and cathodoluminescence (CL) images of selected zircons and dating locations (right) for zircons from volcanic ash bed LM-1in the lower Longmaxi Formation in the Gantianzui outcrop. (B) U–Pb concordia plots (left) and cathodoluminescence (CL) images of selected zircons and dating locations (right) for zircons from volcanic ash bed QL-12 at boundary between the Linxiang Fm. (nodular limestone) and Wufeng Fm. (calcareous shale) in the Muchanggou outcrop.(C) U–Pb concordia plots (left) by the SHRIMP II method and cathodoluminescence (CL) images of selected zircons and dating locations (right) for zircons from volcanic ash bed 2-1 at the top of the Wufeng Formation in the Wangjiawan North outcrop.

Table 5
U–Pb zircon ages using the LA-ICP-MS method from volcanic ash beds QL-1 at boundary between the Linxiang Fm. (nodular limestone) and Wufeng Fm. (calcareous shale) in the Muchanggou outcrop.

Number	^{232}Th(ppm)	^{238}U(ppm)	U/Th	^{207}Pb/^{206}Pb	1δ	^{207}Pb/^{235}U	1δ	^{206}Pb/^{238}U	1δ	^{206}Pb/^{238}U (Ma)	1δ
1	149.2938	261.7736	1.460276754	0.053903267	0.00193	0.538133627	0.0199	0.07208479	0.00124	448.703684	7.46931737
2	142.985	362.1737	2.088580281	0.053775307	0.00166	0.536806944	0.01749	0.07203266	0.00111	448.3901828	6.68779718
3	148.5782	292.3883	1.634199153	0.052747286	0.00145	0.526822696	0.0156	0.07218556	0.00114	449.3095753	6.84354094
4	42.08288	125.8883	2.510168283	0.051887001	0.00145	0.517904309	0.01548	0.07219639	0.00109	449.3746721	6.5700566
5	124.8015	285.3314	1.945330337	0.055071254	0.00112	0.548680622	0.0127	0.07213067	0.0011	448.9795266	6.62861525
6	128.0011	273.7044	1.768094949	0.053693409	0.00096	0.536708294	0.01082	0.07240715	0.00099	450.6416882	5.9413873
7	251.0463	511.3783	1.706414334	0.055287649	0.00082	0.552573527	0.01233	0.07251086	0.00145	451.2650854	8.69940139
8	124.0543	361.0049	2.403740518	0.054027928	0.00091	0.536054292	0.01188	0.07198874	0.00132	448.1260987	7.95667921
9	138.5069	347.8673	2.099246275	0.056268636	0.00087	0.558176057	0.01197	0.07199842	0.00139	448.1842973	8.39202649
10	177.515	374.3678	1.754116639	0.056839919	0.00105	0.565896901	0.01335	0.07206182	0.0013	448.5655129	7.84448273
11	234.5604	645.1188	2.311316214	0.05680093	0.00077	0.565759362	0.0113	0.07218638	0.00134	449.3145047	8.07029484
12	195.1476	446.624	1.915582735	0.056168515	0.00089	0.556392499	0.01142	0.07185999	0.00123	447.3518055	7.38805068
13	225.7711	385.2678	1.446951217	0.056037407	0.00088	0.55920841	0.01173	0.07223389	0.00115	449.6001008	6.9198669
14	202.1886	407.2191	1.706813328	0.055485168	0.00082	0.548834044	0.00933	0.07170747	0.00097	446.4344709	5.831357
15	163.3177	375.2112	1.926206349	0.056472687	0.00097	0.563688562	0.01165	0.07239633	0.00116	450.5766425	6.94745572
16	149.2659	353.1485	1.977270627	0.05609981	0.00098	0.559418277	0.01219	0.07213322	0.00114	448.9948818	6.83820406
17	115.4121	208.521	1.549284792	0.054629735	0.00135	0.545315693	0.0157	0.07214778	0.00115	449.0823811	6.89203074
18	141.8404	337.6968	1.996239894	0.05647496	0.00099	0.562202066	0.01325	0.07204561	0.00131	448.4680401	7.87441796
19	254.3433	441.4867	1.511262431	0.05624296	0.00093	0.560383861	0.01084	0.07199589	0.00092	448.1690937	5.54933322
20	164.2044	314.369	1.979171601	0.057850565	0.00099	0.574283816	0.01196	0.07194505	0.00125	447.8633214	7.54832325
21	165.8462	510.0907	2.616222162	0.056111989	0.00083	0.561459322	0.01205	0.07220557	0.00122	449.4298387	7.34017749
22	160.7262	397.9884	2.094094908	0.056400479	0.0009	0.560924967	0.01054	0.07205558	0.00117	448.5280085	7.04439528
23	175.0646	401.8737	1.920162022	0.054868555	0.00087	0.546411564	0.01069	0.07221595	0.00135	449.4922431	8.12030173
24	185.1183	366.9322	1.652320391	0.059324024	0.00121	0.593463128	0.01504	0.07213998	0.00111	449.0355098	6.67526863
25	426.6838	593.9425	1.384221563	0.061169186	0.00118	0.609396475	0.01442	0.07228812	0.00146	449.9261603	8.80499845
26	180.5667	361.6917	1.660798036	0.056600187	0.00086	0.56495502	0.01011	0.0723009	0.00108	450.002991	6.48137145
27	209.2946	597.8201	2.355364841	0.055866802	0.0009	0.557626106	0.0118	0.07219348	0.00114	449.3571636	6.83317186
28	96.27108	282.988	2.447511011	0.056087555	0.00095	0.558963117	0.01073	0.07222704	0.00111	449.5589422	6.65089828
29	90.12841	230.7029	2.114870961	0.066832687	0.00993	0.700882482	0.12341	0.07375467	0.00126	458.7367536	7.56855122
30	149.2522	361.4208	2.002113289	0.056916447	0.00093	0.567417782	0.01142	0.07219774	0.00102	449.3827923	6.16189964
31	158.0581	429.1825	2.229679043	0.055437068	0.00081	0.552194142	0.01054	0.07220392	0.00113	449.4199546	6.81499746
32	174.1224	368.626	1.765729006	0.054103731	0.00087	0.539159609	0.01124	0.07214089	0.00102	449.0409942	6.12461834
33	198.627	434.5401	1.828601842	0.058697401	0.00109	0.582382131	0.01198	0.07203495	0.00091	448.4039538	5.50148629
34	207.3213	367.5206	1.471268876	0.055172629	0.001	0.551793085	0.01118	0.07220162	0.00139	449.4061254	8.33317606
35	149.6432	357.5755	1.977197455	0.057536455	0.00093	0.578397644	0.01251	0.07192186	0.00146	447.7238894	8.81348961

Table 6
U–Pb zircon ages using the SHRIMPII method from volcanic ash beds 2-1 at the top of the Wufeng Formation in the Wangjiawan Northoutcrop.

Number	^{206}Pb$_c$	U(ppm)	Th(ppm)	^{232}Th/^{238}U	^{206}Pb*(ppm)	^{206}Pb/^{238}U(Ma)		^{207}Pb*/^{206}Pb*	± %	^{207}Pb*/^{235}U	± %	^{206}Pb*/^{238}U	± %
1	0.55	361	459	1.31	22.0	445.9	± 8.4	0.0531	3.1	0.517	3.5	0.0706	1.5
2	0.19	295	316	1.11	18.3	451.6	± 8.4	0.0553	3.4	0.550	3.7	0.0721	1.6
3	0.46	351	214	0.63	21.7	449.3	± 7.5	0.0527	2.8	0.521	3.2	0.0717	1.6
4	–	251	252	1.04	15.6	450.1	± 8.2	0.0547	1.9	0.544	2.5	0.0722	1.6
5	0.18	237	283	1.23	14.9	454.9	± 8.8	0.0547	2.5	0.549	3.0	0.0728	1.6
6	0.27	304	209	0.71	18.2	437.9	± 7.5	0.0567	3.2	0.545	3.6	0.0697	1.6
7	0.29	170	130	0.79	10.9	462.2	± 8.3	0.0625	4.1	0.640	4.4	0.0743	1.6
8	0.50	89	85	0.99	5.13	428.0	± 8.5	0.0558	7.5	0.511	7.8	0.0665	1.8
9	0.27	246	248	1.04	15.2	451.0	± 8.3	0.0537	2.4	0.532	2.8	0.0720	1.6
10	–	160	157	1.02	9.62	437.2	± 8.7	0.0583	3.2	0.565	3.7	0.0703	1.7
11	–	70	57	0.85	4.43	458	± 10	0.0613	4.7	0.628	5.1	0.0743	2.0
12	0.21	386	286	0.77	24.2	454.9	± 8.0	0.0538	2.1	0.541	2.7	0.0729	1.6
13	0.22	375	404	1.11	22.5	433.8	± 8.3	0.0567	2.2	0.545	2.8	0.0697	1.6
14	–	350	376	1.11	20.9	433.0	± 8.5	0.0596	3.1	0.573	3.5	0.0697	1.7
15	0.09	527	304	0.60	32.3	444.6	± 7.4	0.05551	1.6	0.545	2.2	0.0713	1.6
16	–	327	218	0.69	20.0	442.7	± 7.7	0.0609	3.0	0.600	3.4	0.0714	1.6
17	0.65	247	218	0.91	15.5	456.8	± 8.2	0.0507	2.9	0.506	3.3	0.0725	1.6
18	0.33	265	249	0.97	16.9	459.2	± 8.6	0.0565	2.6	0.576	3.1	0.0739	1.6
19	0.10	339	305	0.93	21.0	449.6	± 8.2	0.0574	2.0	0.570	2.6	0.0720	1.6
20	–	481	280	0.60	28.7	435.0	± 7.2	0.05841	1.5	0.560	2.1	0.0695	1.6
21	0.09	551	298	0.56	33.9	445.9	± 7.8	0.0590	2.0	0.582	2.6	0.0715	1.7

Muchanggou are located in different areas of SC (Fig. 1), and the distribution of their ash beds can reveal the scope of volcanic activity in the Late Ordovician period.

Moreover, the main development period of volcanic ash occurred in the Later Ordovician period, and some ash also developed in the early Silurian period (Fig. 9a). In addition, although the three outcrops are located in different areas, the numbers of ash beds are basically the same, with all outcrops having 12–13 beds in the Wufeng Fm. This observation illustrates that the Late Ordovician volcanic activity was a large-scale widespread event in SC rather than a local event. Other studies have also revealed that volcanic ash beds were widely developed in SC (Fig. 9b and c). These volcanic ash beds would play an important role in the study of high-resolution stratigraphic correlations and environmental changes during the OST.

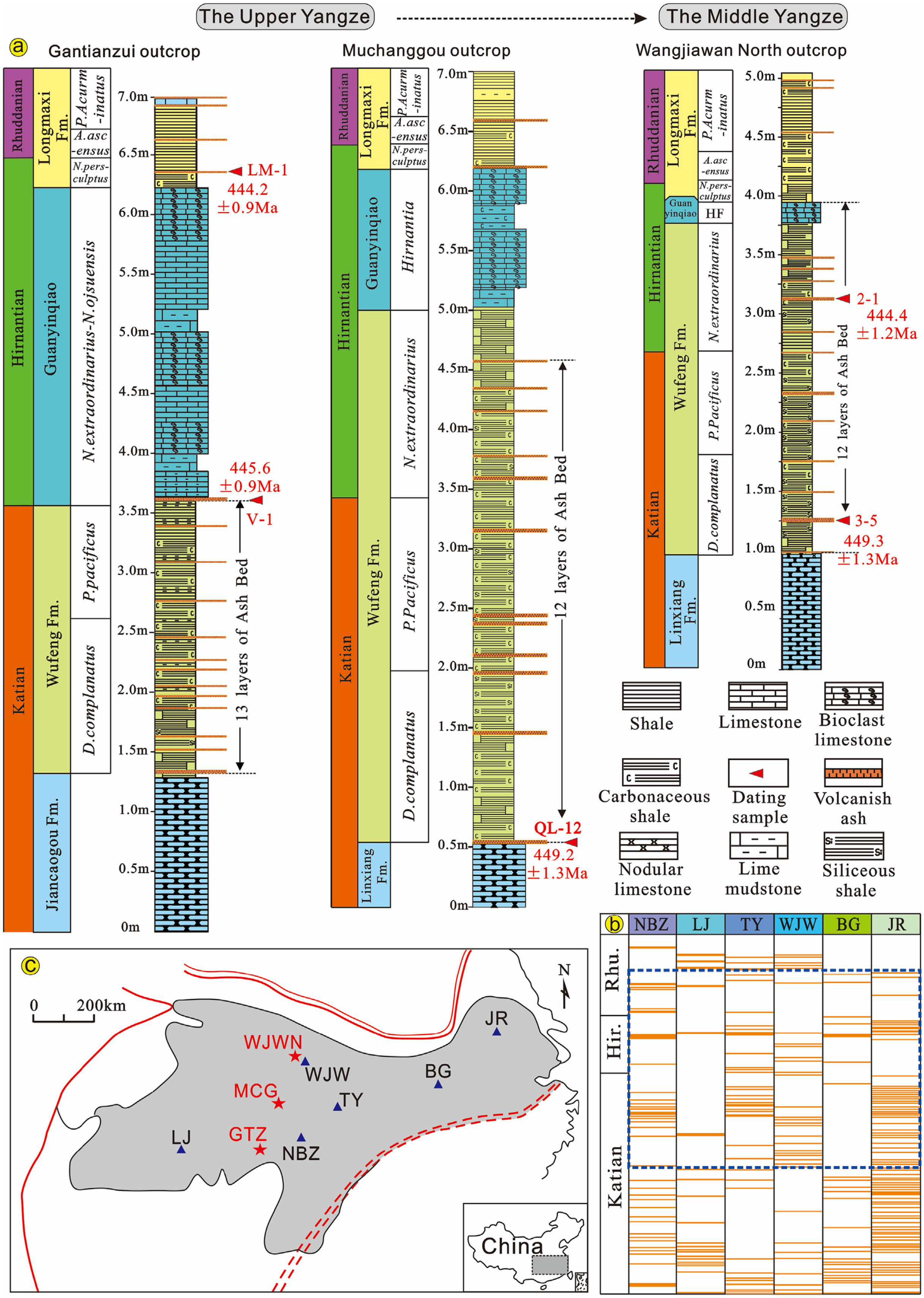

Fig. 9. (a) Comparison of volcanic ash beds of the Upper Ordovician Wufeng Fm.-lower Silurian Longmaxi Fm. in the Middle and Upper Yangtze regions in this study. (b) Volcanic ash beds distribution of the Ordovician-Silurian transition in other outcrops, SC (after Su et al., 2009). (c) the location of mentioned outcrops in SC. Abbreviations: NBZ-Nanbazi; LJ-Luojiang; TY-Taoyuan; WJW-Wanjiawan; BG-Beigong; JR-Jurong; WJWN-Wanjiawan North; MCG- Muchanggou; GTZ-Gantianzui; Hir.-Hirnantian; Rhu.-Rhuddanian.

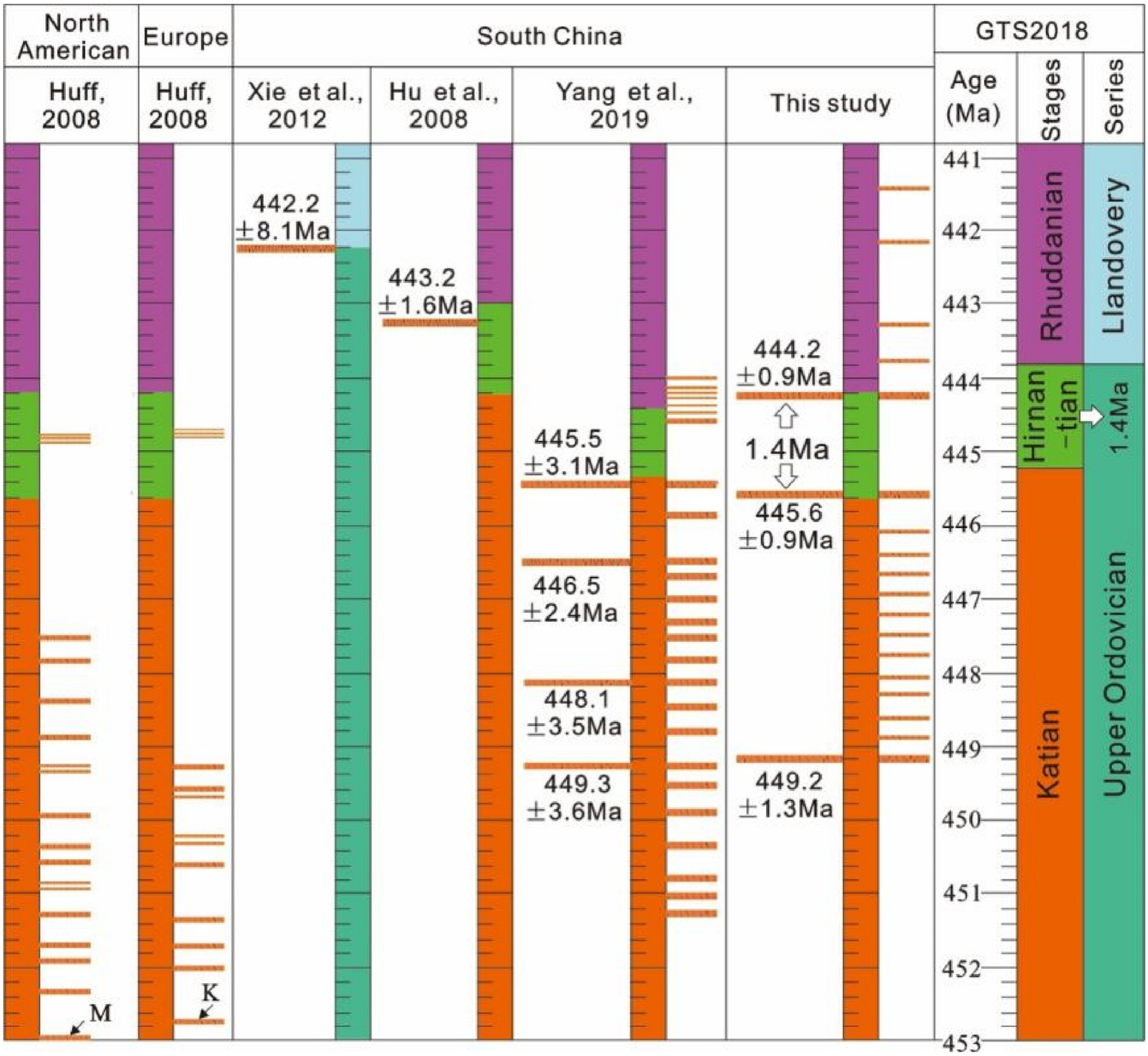

Fig. 10. Comparison of the ages of volcanic ash beds during the OST between SC and GST 2018. Volcanic ash beds from North American and Europe were modified by Huff (2008). M (Millbrig) and K (Kinnekulle) are two famous volcanic ash beds in the world.

Additionally, the Hirnantian ice age was an important global geological event during the OST, which corresponds to the Guanyinqiao bed in SC (Zhang et al., 2019). Fig. 9 shows that the thickness of the Guanyinqiao bed gradually decreases from the Upper Yangtze region to the Middle Yangtze region. The thickness of the bed reaches approximately 5.25 m in Guizhou Province, 3.1 m in Chongqing Province, and less than 1 m in Hubei Province. These results indicate that during the Hirnantian ice age, the sedimentary center of the Guanyinqiao bed was located in Guizhou Province.

5.2. Age constraints for the upper Ordovician-lower Silurian transition in SC

The age of the volcanic ash bed near the boundary represents the beginning time of the overlying sedimentary strata, and if the two formations are in conformity contact, it can reflect the end time of the underlying strata (Gradstein et al., 2008; Zhu et al., 2013). Thus, in this study, the age 449.2 Ma ± 1.3 Ma for the QL-12 volcanic ash bed and the age 449.3 Ma ± 1.3 Ma for the 3–5 volcanic ash bed may basically reflect the beginning time of the Wufeng Fm.; the age 445.6 ± 0.9 Ma for the V-1 volcanic ash bed may basically reflect the beginning time of the Guanyingqiao bed (also the ending time of the Wufeng Fm.); and the age 444.2 Ma ± 0.9 Ma for the LM-1 volcanic ash bed may basically reflect the beginning time of the Longmaxi Fm. (Fig. 9). In addition, the duration of Wufeng Fm. and Guanyingqiao bed can be obtained, which are 3.6 Ma and 1.4 Ma, respectively.

Moreover, we compared the ages in this study to those from previous research results (Fig. 10). The comparison shows that this study could provide more accurate age data than previous studies as well as additional age data to support global comparisons.

First, in this study, the age constraints for OST in SC are basically consistent with that of the whole world. In GST 2018, the age of the Rhuddanian bottom is 444.2 Ma ± 1.5 Ma, and that of the Hirnantian bottom is 445.2 Ma ± 1.4 Ma, whereas in our study, the ages are 444.2 Ma ± 0.9 Ma and 445.6 Ma ± 0.9 Ma respectively. This finding illustrates the reliability of the age data in this study and the consistency of the time-stratigraphic framework between SC and global sites.

Second, during the OST, the Hirnantian stage was a globally comparable event because of the Gondwana ice age, global sea level decline and mass extinction (Zhang et al., 2010). Because of the close relationship between the occurrence of the Hirnantian glacial events and the formation of the cold-water Hirnantian fauna, the beginning of the Hirnantian stage is often determined by the appearance of Hirnantian fauna. *Hirnantia, Hindella, Eostropheodonta, Paromalomena, Kinella,* *Aegiromena, Leptaena* and *Plectothyrella* were common brachiopod fauna in the shallow platform of SC (Zhang et al., 2019). In this study, the age comparison showed that the duration of the Hirnantian stage in SC was 1.4 Ma, which is consistent with the duration determined by the GST 2018(445.2 Ma ± 1.4 Ma-444.2 Ma ± 1.5 Ma).

6. Summary and conclusions

The following conclusions can be drawn from this study:

(1) A comparison of the volcanic ash beds in three different outcrops in SC during OST identified approximately 12–13 ash beds in the Upper Ordovician Wufeng Formation. This observation indicates that during the Late Ordovician period, relatively large-scale volcanic activity occurred in SC.
(2) In SC, the starting time of the Ordovician Wufeng Fm. was approximately 449.2 Ma (449.3 Ma), the starting time of the Ordovician Guanyingqiao bed (the ending time of the Wufeng Fm.) was approximately 445.6 Ma, and the starting time of the Longmaxi Fm. was approximately 444.2 Ma. In addition, the durations of the Wufeng Fm. and Guanyingqiao bed were 3.6 Ma and 1.4Ma, respectively.
(3) The comparison of ash bed distributions from SC and from stratotype sections in Europe and North America suggests volcanic activity during the OST was a global event. It plays an important role in the study of high-resolution stratigraphic correlation and environmental changes during the OST.
(4) Comparisons showed that most of the ages obtained in this study were basically consistent with those for the whole world. The age of the Rhuddanian bottom was 444.2 Ma ± 0.9 Ma, and that of the Hirnantian bottom was 445.6 Ma ± 0.9 Ma. The duration of the Hirnantian stage in SC was 1.4 Ma, which is consistent with the duration determined by GST 2018.

CRediT authorship contribution statement

Xuebin Du: Conceptualization, Methodology, Writing - original draft, Writing - review & editing. **Yongchao Lu:** Supervision. **Dan Duan:** Data curation. **Ke Zhao:** Investigation. **Jixin Jia:** Methodology. **Hang Fu:** Investigation.

Declaration of competing interest

We declare that no conflict of interest exits in the submission of this manuscript, and manuscript is approved by all authors for publication. I would like to declare on behalf of my co-authors that the work described is original research that has not been published previously, and not under consideration for publication elsewhere, in whole or in part. All the authors listed have approved the manuscript that is enclosed.

Acknowledgments

This study is supported by National Science and Technology Major Project (2016ZX05034002, 2016ZX05060004, 2016ZX05027001), Innovative Special Project of Sino-US Intergovernmental Cooperation in Science and Technology (Grant No. 2017YFE0106300), Young Scientists Fund of the National Natural Science Foundation of China (No. 41202086). We would like to thank SINOPEC Jianghan provide important support for core observation and sample collection. This manuscript was greatly improved by helpful comments from several anonymous reviewers and the editors.

Appendix A. Supplementary data

Supplementary data to this article can be found online at https://doi.org/10.1016/j.marpetgeo.2019.104209.

References

Black, L.P., Kamo, S.L., Allen, C.M., Aleinikoff, J.N., Davis, D.W., Korsch, R.J., Foudoulis, C., 2003. T TEMORA 1: a new zircon standard for Phanerozoic U-Pb geochronology. Chem. Geol. 200, 155–170.
Brenchley, P.J., Carden, G.A., Hints, L., Kaljo, D., Marshall, J.D., Martma, T., Meidla, T., Nolvak, J., 2003. High-resolution stable isotope stratigraphy of Upper Ordovician sequences: constraints on the timing of bioevents and environmental changes associated with mass extinction and glaciation. GSA Bulletin 115 (1), 89–104.
Chen, C., Mu, C.L., Zhou, K.K., Liang, W., Ge, X.Y., Wang, X.P., Wang, Q.Y., Zhang, B.S., 2016. The geochemical characteristics and factors controlling the organic matter accumulation of the late Ordovician-early Silurian black shale in the Upper Yangtze Basin, South China. Mar. Pet. Geol. 76, 159–175.
Chen, Q., Fan, J.X., Melchin, M.J., Zhang, L.N., 2014. Temporal and spatial distribution of the Wufeng Formation black shales (upper Ordovician) in South China. GFF 136 (1), 55–59.
Chen, X., Melchin, M.J., Sheets, H.D., Mitchell, C.E., Fan, J.X., 2005. Patterns and processes of latest Ordovician graptolite extinction and recovery based on data from South China. J. Paleontol. 79, 842–861.
Chen, X., Rong, J.Y., Fan, J.X., Zhan, R., Mitchell, C.E., Harper, D.A.T., Melchin, M.J., Peng, P.A., Finney, S.C., Wang, X.F., 2006. The global boundary stratotype section and point (GSSP) for the base of the Hirnantian stage (the uppermost of the Ordovician system). Episodes 29 (3), 183–196.
Chen, X., Rong, J.Y., Fan, J.X., Zhan, R.B., Zhang, Y.D., Li, R.Y., Wang, Y., Mitchell, C.E., Harper, D.A., 2000. A global correlation of biozones across the Ordovician-Silurian boundary. Acta Palaeontol. Sin. 39, 100–114 (in Chinese with English abstract).
Cocks, L.R.M., 2001. Ordovician and Silurian global geography. J. Geol. Soc. 158 (2), 197–210.
Fan, J.X., Melchin, M.J., Chen, X., Wang, Y., Zhang, Y.D., Chen, Q., Chi, Z.L., Chen, F., 2011. Biostratigraphy and geography of the Ordovician-Silurian Longmaxi black shales in South China. Sci. China (Earth Sci.) 54 (12), 1854–1863 (in Chinese with English abstract).
Fan, J.X., Peng, P.A., Melchin, M.J., 2009. Carbon isotopes and event stratigraphy near the Ordovician-Silurian boundary, Yichang, South China. Palaeogeogr. Palaeoclimatol. Palaeoecol. 276, 160–169.
Fu, L.P., Li, Y.X., Song, L.S., Wen, Y.L., 1983. The Silurian system of the west Qinling. J. Stratigr. (4), 16–29 (in Chinese with English abstract).
Gradstein, F.M., Ogg, J.G., van Kranendonk, M., 2008. On the geologic time scale 2008. Newsl. Stratigr. 43, 5–13.
Hammarlund, E.U., Dahl, T.W., Harper, D.A.T., Bond, D.P.G., Nielsen, A.T., Bjerrum, C.J., Schovsbo, N.H., Schönlaub, H.P., Zalasiewicz, J.A., Canfield, D.E., 2012. A sulfidic driver for the end-Ordovician mass extinction. Earth Planet. Sci. Lett. 331–332, 128–139.
Hu, Y.H., Zhou, J.B., Song, B., Li, W., Sun, W.D., 2008. Shrimp zircon U-Pb dating from K-bentonite in the top of Ordovician of Wangjiawan section, Yichang, Hubei, China. Sci. China Ser. D Earth Sci. 51 (4), 493–498.
Huff, W.D., Bergstrom, S.M., Kolata, D.R., Davis, D.W., 1995. Middle Ordovician K-Bentonites discovered in the Precordillera of Argentina: geochemical and paleogeographical implications. Pacific Section SEPM. In: Ordovician Odyssey: Short Papers for the Seventh International Symposium on the Ordovician System, pp. 343–349.
Huff, W.D., 2008. Ordovician K-bentonites: issues in interpreting and correlating ancient tephras. Quat. Int. 178, 276–287.
Huff, W.D., Dronov, A.V., Sell, B., Kanygin, A.V., Gonta, T.V., 2014. Traces of explosive volcanic eruptions in the upper Ordovician of the Siberian Platform. Est. J. Earth Sci. 63 (4), 244–250.
Kump, L.R., Arthur, M.A., 1999. Interpreting carbon-isotope excursions: carbonates and organic matter. Chem. Geol. 161, 181–198.
Li, P., Hu, Z.X., Wu, L., Du, X.F., Zong, W., Zhou, F., Mao, Q.X., 2017. Discovery of bentonite in Silurian Shamao Formation in western Hubei: implication on geochronology of U-Pb zircon. Geol. Sci. Technol. Inf. 36, 1–9 (in Chinese with English abstract).
Lu, Y.B., Huang, C.J., Jiang, S., Zhang, J.Y., Lu, Y.C., Liu, Y., 2019. Cyclic late Katian through Hirnantian glacioeustasy and its control of the development of the organic-rich Wufeng and Longmaxi shales, South China. Palaeogeogr. Palaeoclimatol. Palaeoecol. 526, 96–109.
Lu, Y.B., Ma, Y.Q., Wang, Y.X., Lu, Y.C., 2017. The sedimentary response to the major geological events and lithofacies characteristics of Wufeng Formation-Longmaxi Formation in the Upper Yangtze area. Earth Sci. 2 (7), 1169–1184 (in Chinese with English abstract).
Ludwig, K.R., 2002. SQUID 1.02, a User's Manual, vol. 2. Berkeley Geochronology Center Special Publication, pp. 22.
Ludwig, K.R., 2012. User's Manual for Isoplot 3.75: a Geochronological Toolkit for Microsoft Excel. Berkeley Geochronology Center Special Publication, USA No 5.
Luo, H., He, R.L., Pan, L.K., Yang, C., Yu, G.F., 2016. LA-ICP-MS zircon U-Pb age and its significance of late Ordovician-early Silurian Longmaxi bentonite. Resour. Environ. Eng. 30 (1), 547–550 (in Chinese with English abstract).
Ross, R.J., Naeser, C.W., 1984. The Ordovician time scale-New refinement. InAspects of the Ordovician system. In: Bruton, D.L. (Ed.), Paleontological Contribution from the University of Oslo, pp. 5–10 No.295.
Shen, J., Algeo, T.J., Chen, J.B., Planavsky, N.J., Feng, Q.L., Yu, J.X., Liu, J.L., 2019. Mercury in marine Ordovician/Silurian boundary sections of South China is sulfide-hosted and non-volcanic in origin. Earth Planet. Sci. Lett. 511, 130–140.
Shu, Y., Lu, Y.C., Liu, Z.H., Wang, C., Mao, H.W., 2017. Development characteristics of bentonite in marine shale and its effect on shale reservoir quality: a case study of Wufeng Formation to member 1 of Longmaxi Formation, Fuling area. Acta Pet. Sin.

38, 1371–1380 (in Chinese with English abstract).
Su, W.B., Huff, W.D., Ettensohn, F.R., Liu, X.M., Zhang, J.E., Li, Z.M., 2009. K-bentonite, black-shale and flysch successions at the Ordovician-Silurian transition, South China: possible sedimentary responses to the accretion of Cathaysia to the Yangtze Block and its implications for the evolution of Gondwana. Gondwana Res. 15 (1), 111–130.
Su, W.B., He, L.Q., Wang, Y.B., Gong, S.Y., Zhou, H.Y., 2003. K-bentonite beds and high-resolution integrated stratigraphy of the uppermost Ordovician Wufeng and the lowest Silurian Longmaxi Formations in South China. Sci. China (Ser. D) 46 (11), 1121–1133 (in Chinese with English abstract).
Su, W.B., He, Y.Q., Wang, Y.B., Gong, S.Y., Zhou, H.Y., 2002. Bentonite and high resolution stratigraphy at the bottom of Wufeng Formation and Longmaxi Formation of Ordovician-Silurian in South China. Sci. China (Ser. D) 32 (3), 207–209 (in Chinese with English abstract).
Sun, S.S., Rui, Y., Dong, D.Z., Shi, Z.S., Bai, W.H., Ma, C., Zhang, L.F., Wu, J., Chang, Y., 2018. Paleogeographic evolution of the late Ordovician-early Silurian in upper and middle Yangtze regions and depositional model of shale. Oil Gas Geol. 39, 1–20 (in Chinese with English Editor).
Svensen, H.H., Hammer, Ø., Corfu, F., 2015. Astronomically forced cyclicity in the upper Ordovician and U-Pb ages of interlayered tephra, Oslo Region, Norway. Palaeogeogr. Palaeoclimatol. Palaeoecol. 418, 150–159.
Thompson, C.K., Kah, L.C., Astini, R., Bowring, S.A., Buchwaldt, R., 2012. Bentonite geochronology, marine geochemistry, and the great Ordovician biodiversification event (GOBE). Palaeogeogr. Palaeoclimatol. Palaeoecol. 321–322, 88–101.
Wan, Y.S., Dong, C.Y., Liu, D.Y., Kröner, A., Yang, C.H., Wang, W., Du, L.L., Xie, H.Q., Ma, M.Z., 2012. Zircon ages and geochemistry of late Neoarchean syenogranites in the North China Craton: a review. Precambrian Res. 222–223, 265–289.
Wang, G.X., Zhan, R.B., Percival, I.G., 2019a. The end-Ordovician mass extinction: a single-pulse event? Earth Sci. Rev. 192, 15–33.
Wang, X.F., Zeng, Q.L., Zhou, T.M., Ni, S.Z., Xu, G.H., Li, Z.H., 1983. Biostratigraphy of the boundary on the Ordovician-Silurian in the eastern region of the three gorges, China. Sci. China (Ser. B) 13 (12), 65–74 (in Chinese).
Wang, Y.M., Li, X.J., Wang, H., Jiang, S., Chen, B., Ma, J., Dai, B., 2019b. Developmental characteristics and geological significance of the bentonite in the upper Ordovician Wufeng -lower Silurian Longmaxi Formation in eastern Sichuan basin, SW China. Pet. Explor. Dev. 46 (4), 653–665 (in Chinese with English Editor).
Wiedenbeck, M., Allé, P., Corfu, F., Griffin, W.L., Oberli, F.M.M., Vonquadt, A., Roddick, J.C., Spiegel, W., 1995. Three natural zircon standards for U-Th-Pb, Lu-Hf, trace element and REE analyses. Geostand. Newsl. 19, 1–23.
Williams, I.S., 1998. U-Th-Pb geochronology by ion microprobe. In: McKibben, M.A., Shanks IIIW.C., Ridley, W.I. (Eds.), Applications of Microanalytical Techniques to Understanding Mineralising Processes. Society of Economic Geologists, Colorado, pp. 1–35.
Wu, L.Y., Lu, Y.C., Jiang, S., Liu, X.F., He, G.S., 2018. Effects of volcanic activities in Ordovician Wufeng-Silurian Longmaxi period on organic-rich shale in the upper Yangtze area, South China. Pet. Explor. Dev. 45 (5), 806–816 (in Chinese with English abstract).
Xie, S.K., Wang, Z.J., Wang, J., Zhuo, J.W., 2012. LA-ICP-MS zircon U-Pb dating of the bentonites from the uppermost part of the Ordovician Wufeng Formation in the Haoping section, Taoyuan, Hunan. Sediment. Geol. Tethyan Geol. 32 (4), 65–69 (in Chinese with English abstract).
Yan, D., Wang, H., Fu, Q.L., Chen, Z.H., He, J., Gao, Z., 2015a. Geochemical characteristics in the Longmaxi Formation (early Silurian) of South China: implications for organic matter accumulation. Mar. Pet. Geol. 65, 290–301.
Yan, D., Wang, H., Fu, Q.L., Chen, Z.H., He, J., Gao, Z., 2015b. Organic matter accumulation of late Ordovician sediments in North Guizhou Province, China: sulfur isotope and trace element evidence. Mar. Pet. Geol. 59, 348–358.
Yang, S.C., Hu, W.X., Wang, X.L., Jiang, B.Y., Yao, S.P., Sun, F.N., Huang, Z.C., Zhu, F., 2019. Duration, Evolution, and Implications of Volcanic Activity across the Ordovician-Silurian Transitionin the Lower Yangtze Region, vol. 518. EarthandPlanetaryScienceLetters, South China, pp. 13–25.
Zhang, Y.D., Zhan, R.B., Fan, J.X., Cheng, J.F., Liu, X., 2010. Principal aspects of the Ordovician biotic radiation. Sci. China (Earth Sci.) 53 (3), 382–394.
Zhang, Y.D., Zhan, R.B., Zhen, Y.Y., Wang, Z.H., Yuan, W.W., Fang, X., Ma, X., Zhang, J.P., 2019. Ordovician integrative stratigraphy and timescale of China. Sci. China Earth Sci. 62, 61–88.
Zhu, Z.Y., Jiang, S.Y., Liu, G.X., Zhao, K.D., 2013. Precise dating of the middle Permian: zircon U-Pb geochronology from volcanic ash beds in the basal Gufeng Formation, Yangtze region, South China. Gondwana Res. 23, 1599–1606.